MINNESOTA GEOLOGICAL SURVEY
PRISCILLA C. GREW, *Director*

MANGANIFEROUS ZONES IN EARLY PROTEROZOIC IRON-FORMATION IN THE EMILY DISTRICT, CUYUNA RANGE, EAST-CENTRAL MINNESOTA

G.B. Morey, D.L. Southwick, and Shawn P. Schottler

Report of Investigations 39
ISSN 0076-9177

UNIVERSITY OF MINNESOTA
St. Paul — 1991

MANGANIFEROUS ZONES IN EARLY PROTEROZOIC IRON-FORMATION IN THE EMILY DISTRICT, CUYUNA RANGE, EAST-CENTRAL MINNESOTA

CONTENTS

ILLUSTRATIONS

TABLES

MANGANIFEROUS ZONES IN EARLY PROTEROZOIC IRON-FORMATION IN THE EMILY DISTRICT OF THE CUYUNA IRON RANGE, EAST-CENTRAL MINNESOTA

By

G.B. Morey, D.L. Southwick, and Shawn P. Schottler

ABSTRACT

Early Proterozoic strata in the Emily district of the Cuyuna iron range of east-central Minnesota unconformably overlie older folded rocks of the North range (North range group). They are correlative with strata of the Animikie Group on the Mesabi iron range, which consist of a lower quartz arenitic sequence (Pokegama Quartzite), an intermediate iron-rich sequence (Biwabik Iron Formation), and an upper feldspar-rich, graywacke-shale sequence (Virginia Formation). In the Emily district, however, the stratigraphic position of the Biwabik Iron Formation is occupied by three units of iron-formation separated by intervening sequences of black shale. Manganese occurs in the lowest iron-rich unit (informally termed Unit A of the Ruth Lake area).

Unit A can be divided into six lithotopes. They are: (1) an epiclastic lithotope of quartz-rich siltstone and shale; (2) a mixed epiclastic jaspery chert lithotope; (3) an oolitic and pisolitic lithotope; (4) a thick-bedded lithotope of cherty or granular iron-formation; (5) a mixed thick- and thin-bedded lithotope characterized by thick intervals of slaty or non-granular iron-formation; and (6) a ferruginous chert lithotope. In general, lithotopes 1, 2, and 3 have shallow-water attributes, whereas lithotope 6 was deposited in quieter, presumably deeper water. Lithotopes 4 and 5 interfinger, and thus were deposited in generally similar sedimentological regimes in water of intermediate depth that was variably affected by currents. Unit A was deposited during two trangressive-regressive cycles in a basin that deepened to the north. Well-rounded grains of terrigenous quartz, which persist throughout lithotopes 1-5, imply that much of the sedimentation occurred relatively close to strandline.

Although Unit A in the Ruth Lake area has many mineralogical and chemical attributes typical of "ordinary" iron-formation, it contains manganese at levels that are one or two orders of magnitude larger than the norm. Manganese oxides are distributed throughout lithotopes 1-5 as disseminated grains, as thin pods or lenses, and as layers as thick as 1.5 meters that typically contain about 10 percent Mn, but some contain as much as 20-30 percent. In addition, Unit A contains two major, laterally persistent zones about 15 to 18 meters thick, in which the manganese tenor has been enriched to the 10-50 percent range by secondary processes. Both enriched zones more or less coincide with stratigraphic positions occupied by the oolitic-pisolitic lithotope. They contain various proportions of psilomelane, cryptomelane, hematite, and quartz. Goethite and manganite may be locally abundant, and where they occur they are secondary phases that formed during a period of intense chemical weathering in Late Jurassic or Early Cretaceous time.

Primary stratigraphic, textural, and mineralogic attributes of the Ruth Lake strata correspond to those used by James (1955) to define the oxide (hematite) facies of iron-formation. The hematite and chert are syngenetic, but the manganese oxides are more likely epigenetic. It is inferred that the manganese oxides were deposited in porous and permeable parts of the Ruth Lake sequence by a reflux process involving reducing solutions that leached manganese from older rocks of the North range group. The principal mechanisms for manganese concentration are inferred to have been early diagenetic, and therefore to have operated in Early Proterozoic time. Mesozoic weathering phenomena have been imposed on the rocks and have caused some redistribution of manganese. The abundance of manganese makes the Ruth Lake area in the Emily district a potential target for in situ mining techniques currently being developed by the U.S. Bureau of Mines and the Mineral Resources Research Center of the University of Minnesota.

INTRODUCTION

Ever since their discovery in 1904, the iron-formations and associated ore deposits of the Cuyuna iron range in east-central Minnesota (Fig. 1) were known to be manganiferous. Ferromanganese ores were mined from several places on the North range from 1911 to 1984, and stockpiled ore is still being shipped for making specialty steel. The presence of this manganese resource sets the Cuyuna range apart from other iron-mining districts of the Lake Superior region.

Between the late 1940s and the mid-1950s there was much exploratory drilling in the gap between the west end of the Mesabi range and the Cuyuna range. This activity led to the discovery of iron-rich strata in the so-called Emily district (Fig. 1), which were described in some detail by Marsden (1972). Our reanalysis of core samples and associated drilling records during the preparation of a regional map of east-central Minnesota (Southwick and others, 1988) led us to recognize that iron-formation in the Emily district was characterized by stratigraphic intervals of 1.5 meters or more that contain as much as 50 percent manganese. A preliminary examination of these materials showed that they were significantly different from the manganiferous iron-formations of the North range as described by Schmidt (1963).

The emphasis of this report is on the geologic factors that seem to control how the manganese is distributed in one part of the Emily district, the so-called Ruth Lake area in sections 20 and 21, T. 138 N., R. 21 W. What follows is a preliminary analysis of the structural and stratigraphic attributes of the iron-rich host rocks, together with a summary of their textural, mineralogical, and sedimentological features. A preliminary analysis also is given of tenor, extent, location, and origin of the manganese-bearing materials that have been recognized in the iron-formation.

The ultimate economic utilization of the manganese deposits in the Emily district is dependent on metallurgical and beneficiation techniques that must be designed specifically for the potential ores. Toward that goal, this report, if nothing else, should call attention to deficiencies in the present geological data base.

REGIONAL GEOLOGIC SETTING

The Cuyuna iron range (Fig. 1) is about 160 km southwest of Duluth, Minnesota in Aitkin, Cass, Crow Wing, and Morrison Counties. It is part of an Early Proterozoic geologic terrane which occupies much of east-central Minnesota. The Cuyuna iron range is traditionally divided into three districts—the Emily district, the North range, and the South range. The Emily district extends from the Mississippi River northward through Crow Wing County and into southern Cass County, and comprises an area of about 1165 square kilometers. Although exploratory drilling has been extensive in the Emily district, mining never commenced. The North range, a much smaller area about 19 km long and 8 km wide, is near the cities of Crosby and Ironton in Crow Wing County. Although relatively small, the North range was the principal site of mining activity, which had largely ceased by 1975. The South range, where only a few underground mines were operated in the 1910s-20s, comprises an area of northeast-trending, generally parallel belts of iron-formation extending from near Randall in Morrison County northeast for about 100 km. In addition to the three named districts, numerous linear magnetic anomalies occur to the east of the range proper, and may indicate other, but as yet poorly defined, beds of iron-formation.

East-central Minnesota, including all of the Cuyuna range, is a generally flat area dominated by constructional glacial deposits related to several continental ice sheets which covered the area in late Pleistocene time. The present drainage system is poorly integrated; the area therefore is swampy and the water table is very near the mean level of the intricately meandering Mississippi River. Because of the high water table and relatively poor drainage, the mines of the Cuyuna range filled with water to within several meters of the land surface soon after mining and pumping ceased.

The glacial deposits, which in places are as thick as 150 meters, obscure much of the bedrock. Natural bedrock outcrops are very sparse, and exposures that once existed in the various mines are no longer available for study. Therefore structural and stratigraphic relationships in the bedrock must be pieced together from subsurface exploration records obtained from old exploration projects that focused on the identification and characterization of various magnetic anomalies. In fact, the Cuyuna range was one of the first, if not the first, mining districts in the United States to be discovered by geophysical methods and supplementary exploratory drilling. In short, understanding the geology of the Cuyuna range is an exercise in subsurface stratigraphic and structural analysis.

Early geologic studies pertinent to the Cuyuna range in particular include those of Harder and Johnston (1918); Zapffe (1933); Woyski (1949); Grout and Wolff (1955); Schmidt (1963); Marsden (1972); and Keighin and others (1972). These works were incorporated by Morey (1978) in a regional geologic synthesis that was founded on the stratigraphic premise that a single major iron-rich interval tied together the Emily district, the North range, and the South range (Fig. 2). The tectonic framework of east-central Minnesota as mapped by Morey and others (1981) was also based on that premise and on the assumption that mainly vertical tectonic processes were responsible for a series of large synclines and anticlines in a pattern of superimposed interference folds. That mapping was guided in areas of no

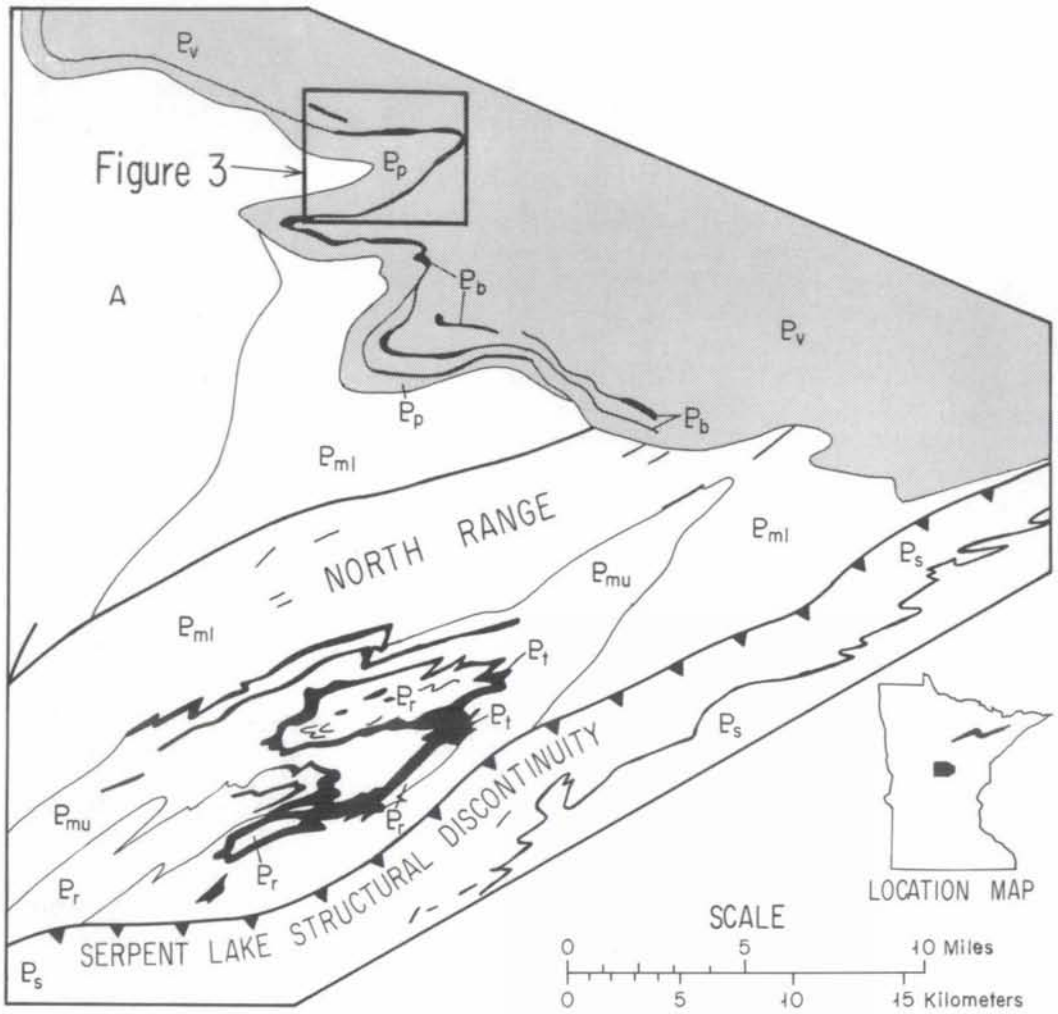

EXPLANATION

Animikie Group

P_v Virginia Formation

P_b Iron-formation

P_p Pokegama Quartzite

North range group

P_r Rabbit Lake Formation

P_t Trommald Formation

P_m Mahnomen Formation, including lower and upper members

P_{ml} P_s Sedimentary rocks of the Mille Lacs Group, undivided (P_{ml}) and sedimentary and volcanic rocks at the South range structural panel, undivided

A Archean rocks, undivided

Figure 1. Generalized geologic map of the Cuyuna iron range (modified from Southwick and others, 1988). Rocks of the Animikie Group unconformably overlie those of the North range group, which are separated from rocks of the South range by the Serpent Lake structural discontinuity. The western end of the Biwabik Iron Formation of the Mesabi range is about 25 km north of the area of this figure.

geologic data by the gravity (Krenz and Ervin, 1977; McGinnis and others, 1977, 1978) and magnetic (Bath and others, 1964, 1965) data that were available in the mid-1970s.

In the 9 years since the work of Morey and others (1981), the body of geophysical data and drill-hole information pertaining to the area has grown substantially. A new high-resolution aeromagnetic survey of the region has been flown (Chandler, 1983a, 1983b, 1983c, 1985), and computer-prepared derivative maps and theoretical models based on the aeromagnetic data (Carlson, 1985; Chandler and Malek, 1991) have extended the utility of the potential field data beyond qualitative interpretation. Scientific test drilling was undertaken by the Minnesota Geological Survey in order to determine the sources of selected aeromagnetic anomalies and anomaly patterns. During that period, several of the iron-mining companies formerly active in the area released several thousand exploration records and drill cores. These old data have been especially valuable in deciphering the complex structure of the Emily district where public information on the geology had been scarce.

Three major insights regarding the geology of the Cuyuna range have emerged from the recently acquired data. First, there is clear evidence that iron sedimentation occurred at several different times under varying geological conditions. Major iron-formations are associated stratigraphically with volcanic rocks and black shale in the South range, with black shale and graywacke in the North range, and with mostly shallow-water deposits of sandstone and deeper water shales in the Emily district.

Second, the iron-rich strata of the Emily district are correlative (Fig. 2) with the Biwabik Iron Formation of the Mesabi range, as inferred by Marsden (1972) and Morey (1978). They and the other sedimentary rocks of the well-known Animikie Group occur above a major deformed unconformity that cuts across the previously deformed and somewhat older sedimentary and volcanic rocks of the North range, which form part of a locally twice-deformed sequence. Therefore the rocks of the North range and the Emily district cannot be correlative, but are separate stratigraphic entities. As defined by Schmidt (1963), the stratigraphic units of the North range are a quartz-rich sandstone-siltstone sequence named the Mahnomen Formation; a middle iron-rich and locally manganese-rich sequence assigned to the Trommald Formation; and an upper graywacke-shale interval called the Rabbit Lake Formation. Southwick and others (1988) referred to it informally as the North range group (small g), with the understanding that a formal name may be justified at a later time.

Third, Southwick and others (1988) recognized several geophysically defined structural discontinuities within and southeast of the South range. They mark demonstrable contrasts in metamorphic grade, structural style, and lithic components. One of the most pronounced of the discontinuities, the Serpent Lake structural discontinuity, passes along the south edge of the North range. It is interpreted as a tectonic boundary, probably involving major thrust faults between slices of folded rocks. Thus it seems fairly certain that the iron-rich strata of the South range are not correlative with either the Trommald Formation of the North range or the iron-rich strata of the Emily district.

The fact that iron-formation occurs within three different stratigraphic and structural contexts in the Cuyuna iron range is of considerable importance. Because we now recognize that the Emily district, the North range, and the South range are separate entities, we can no longer develop regional syntheses that extrapolate mineralogical and structural attributes from one entity to another.

THE EMILY DISTRICT

The Emily district at the far northern end of the Cuyuna iron range defines the southwestern closure of the Animikie basin as established by Southwick and others (1988). The rocks of the basin are particularly well studied on the Mesabi range where the sedimentary fill consists of the Pokegama Quartzite, the Biwabik Iron Formation, and the Virginia Formation, all assigned to the Animikie Group (Morey, 1983).

Stratigraphic and structural relationships are imperfectly known between the western end of the Mesabi range and the Emily district (Fig. 1), because the glacial materials are very thick. Nonetheless aeromagnetic patterns and scattered drill-hole information lead to several conclusions: The Biwabik Iron Formation thins to the west along the Mesabi range, and apparently continues to thin as it curves around the western end of the Animikie basin. In the Emily district proper, the stratigraphic position of the Biwabik is occupied by three broadly lenticular units of iron-formation that are separated from one another by intervening sequences of black shale. The lower unit was mapped as the Biwabik by Marsden (1972), who referred to the two higher iron-formations as the "Emily iron-formation member of the Rabbit Lake Formation" (Fig. 2). Morey (1978) proposed that the Biwabik of the Emily district, as defined by Marsden (1972), correlated with the Trommald Formation of the North range, as defined by Schmidt (1963). Morey also correlated the Emily Member of the Rabbit Lake Formation, as defined by Marsden (1972), with an unnamed unit of iron-formation in the lower part of the Virginia Formation that was first recognized by White (1954). In this scheme, the third iron-formation of the Emily district was yet another unnamed unit in the Virginia Formation. In contrast to this scheme, Southwick and others (1988) have suggested that all three iron-rich lenses in the Emily district together occupy the same approximate stratigraphic position as that of the Biwabik Iron Formation on the Mesabi range.

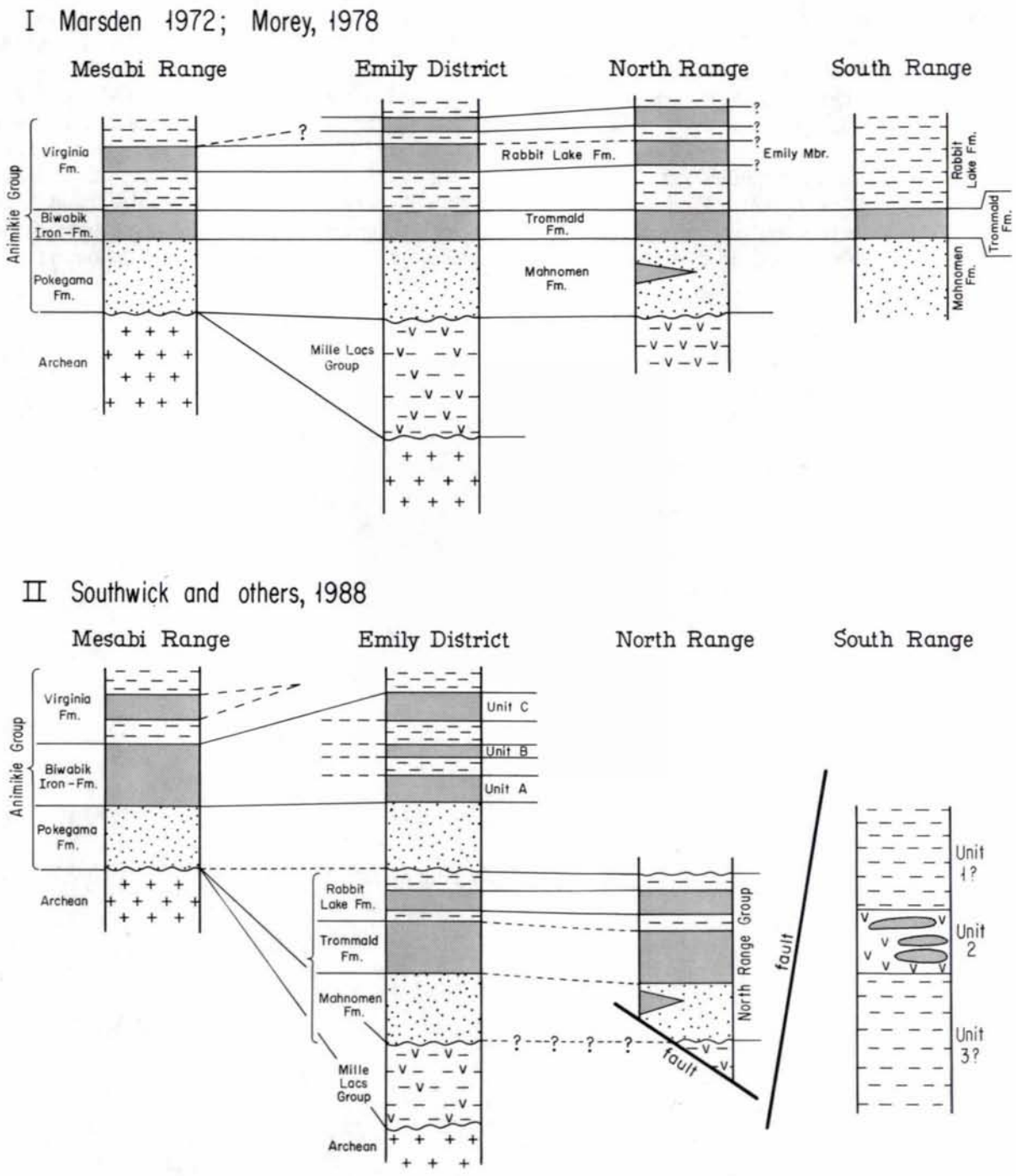

Figure 2. Comparison of stratigraphic correlation schemes of iron-rich strata in east-central Minnesota by Marsden (1972) and Morey (1978) with that by Southwick and others (1988).

The map geometry of the Emily district shown in Figure 1 was first inferred by Marsden (1972) from geophysical and drilling data then held as proprietary information by United States Steel Corporation. Subsequently U.S. Steel donated much of that information, together with core material, to the State of Minnesota and it is now available for study at the offices of the Department of Natural Resources, Division of Minerals, in Hibbing.

Regionally, the main bowl of the Animikie basin is a broad synclinorium that plunges to the east (Marsden, 1972; Southwick and others, 1988). The intensity of deformation increases systematically from north to south across the basin. From near their northern margin, just south of the Mesabi range, strata of the Animikie Group dip gently southward and the unconformity between them and the Archean basement is relatively undisturbed. Incipient slaty cleavage first appears about 15 km south of the Mesabi range, where the rocks are thrown into a series of broad, open, east-trending folds that have vertical axial planes. This structural style persists into the Emily district, where map patterns strongly imply open folding of the Animikie Group and the presence of a weakly deformed unconformity beneath the Animikie Group that is cut onto older folded rocks of the North range (Fig. 1). This unconformable relationship is supported geophysically by an analysis of gravity and magnetic data (Chandler and Malek, 1991) that detected anomaly patterns characteristic of the folded rocks of the North range far northeast of their surface termination.

The iron-formations and associated rocks of the Emily district have been pervasively oxidized and leached, particularly along the hinges of folds where the rocks tend to be more closely fractured. However, oxidation and leaching

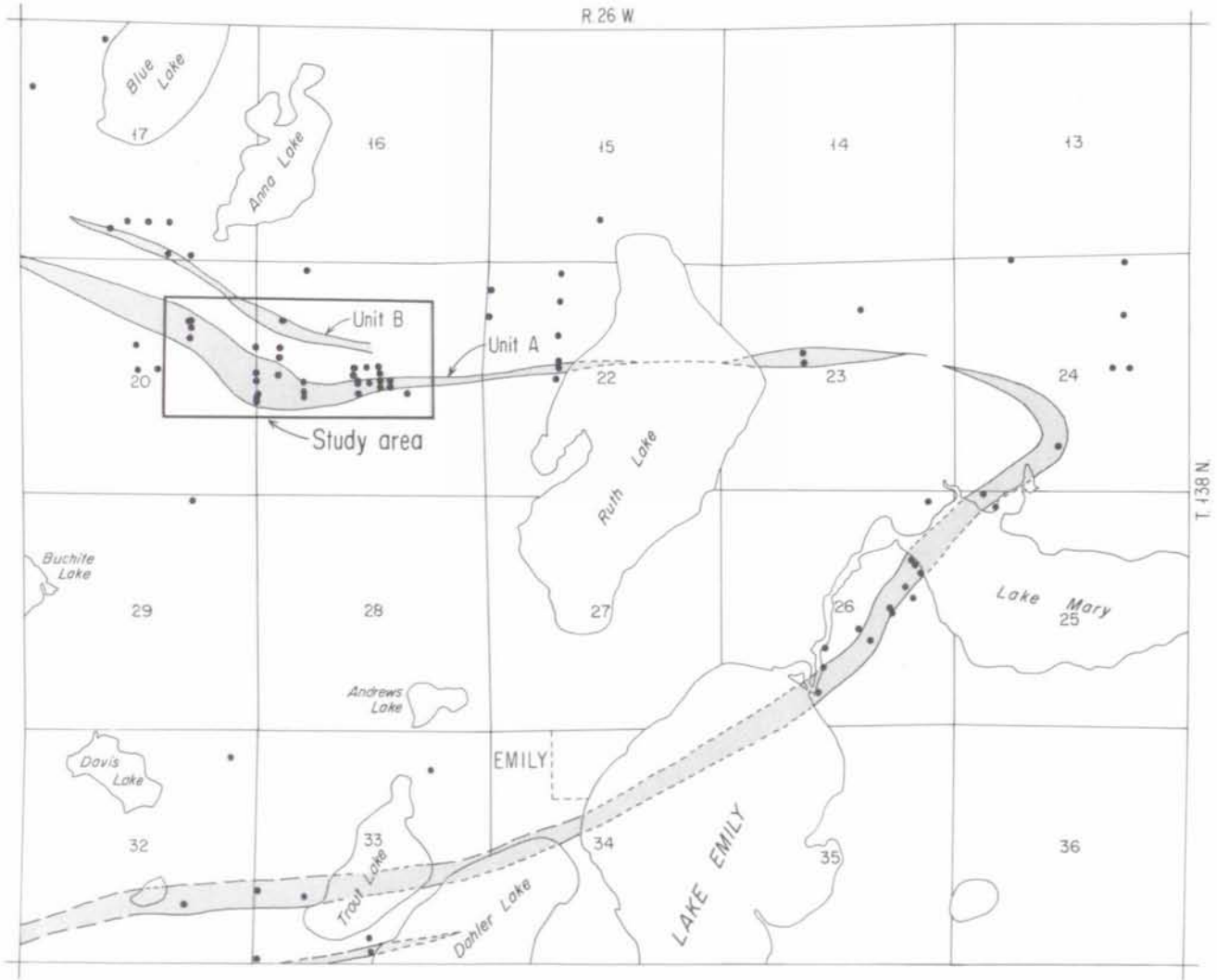

Figure 3. Generalized geologic map of the south half of T. 138 N., R. 26 W. in the Emily district showing the inferred distribution of iron-rich strata (stippled) in the Emily-Ruth Lake study area (Figs. 4, 5, and 16).

are quite variable from place to place. In some drill holes, fresh rock was encountered at depths of only a few meters below the bedrock surface, whereas thoroughly oxidized and partially leached iron-formation has been encountered elsewhere at depths of nearly 240 meters (Marsden, 1972).

Although manganiferous strata were reported previously from various places in the Emily district (e.g., Marsden, 1972; Beltrame and others, 1981), they never were studied in detail, partly because of the pervasive alteration, partly because of the relatively thick glacial cover, and also partly because the resource was considered to be an extension of that in the better known North range (Schmidt, 1963). An analysis of exploration records and nearly 1000 meters of core and churn-drill cuttings from 20 holes (Fig. 3) shows that the Ruth Lake area lies along the north limb of an east-northeast plunging anticline. The iron-formation strikes to the east and dips 15° to 40° to the north (Fig. 4). The iron-formation seems to flatten toward the north, away from the anticlinal axis. This implies that the north limb of the regional fold has a riser-and-tread configuration in the down-dip direction or that the north limb flattens to the north. The iron-formation also is broken by a conjugate set of north-northeast- and west-northwest-striking faults that have apparent displacements on the order of meters or tens of meters.

STRATIGRAPHIC SETTING AT RUTH LAKE

The stratigraphic conclusions of this study are summarized in a series of cross and longitudinal sections (Figs. 5, 6, and 7) which are based in part on the lithologic classifications of U.S. Steel geologists recorded as the original drilling progressed. Unit A can be divided into six distinct lithotopes. They are: (1) Epiclastic lithotope composed mainly of quartz sand and silt grains; (2) Mixed lithotope of epiclastic sandstone and siltstone interlayered with chert; (3) Oolitic or pisolitic iron-formation; (4) Thick-bedded granular iron-formation; (5) Mixed thick-bedded and thin-bedded iron-formation; and (6) Ferruginous chert. Lithotopes 1 and 2 are complexly interstratified and compose a basal unit that marks a change from epiclastic sedimentation in Pokegama time to chemical precipitation in Unit A time. Lithotope 6 occurs predominantly in the upper part of Unit A where it grades upward into the

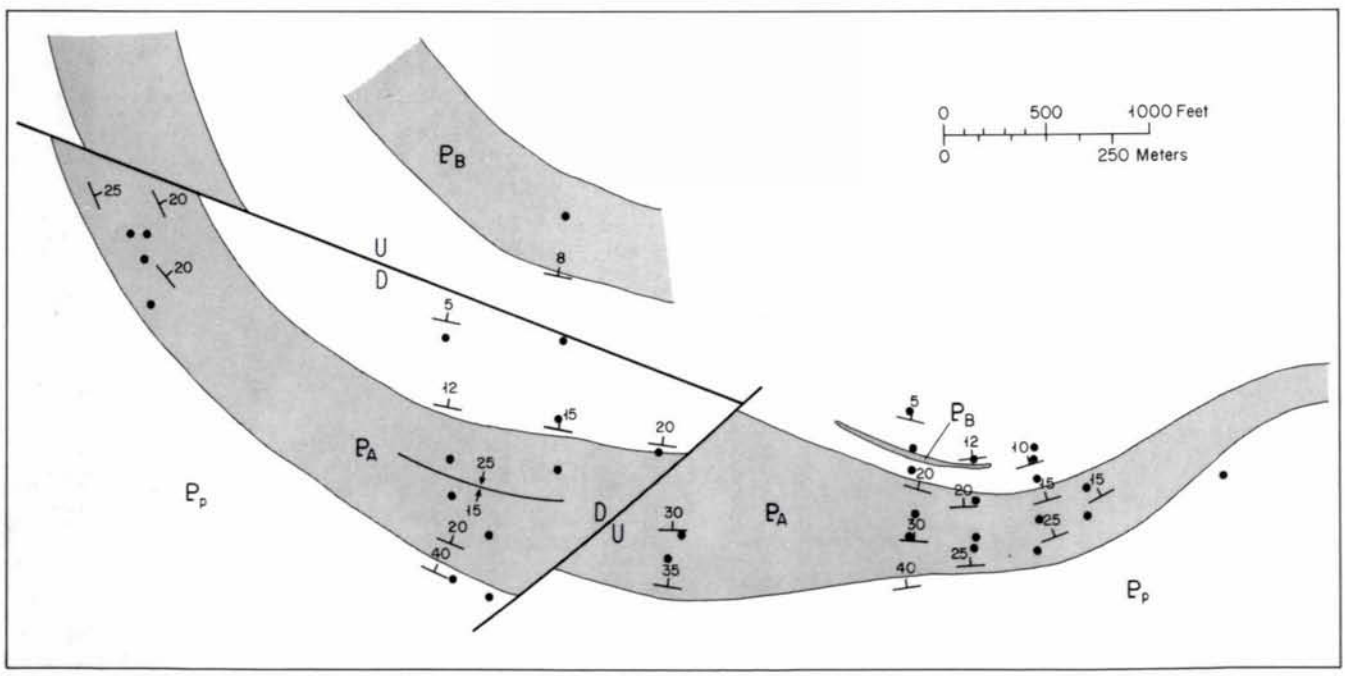

Figure 4. Geologic map of the Ruth Lake area in parts of sections 20 and 21, T. 138 N., R. 26 W. Units PA and PB are iron-rich strata; Pp is the Pokegama Quartzite.

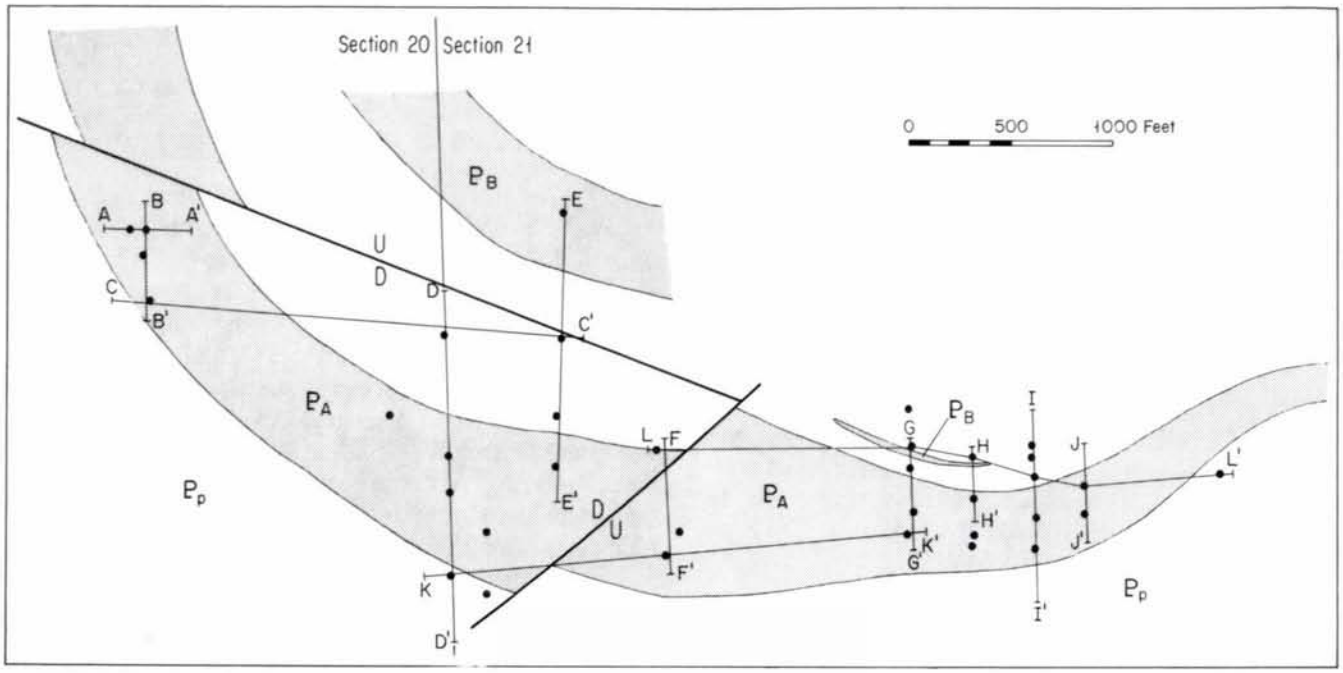

Figure 5. Geologic Map of the Ruth Lake area showing the locations of longitudinal sections in Figure 6 and cross sections in Figure 7.

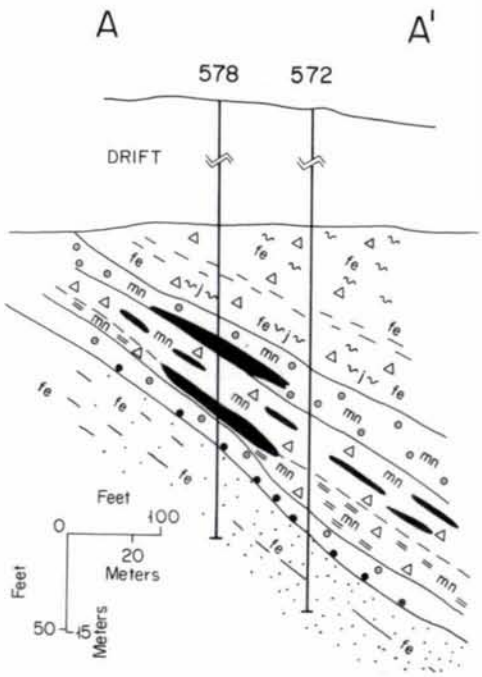

Figure 6. Selected longitudinal sections showing the inferred distribution of lithotopes in Unit A at Ruth Lake. See Figure 5 for locations of longitudinal sections.

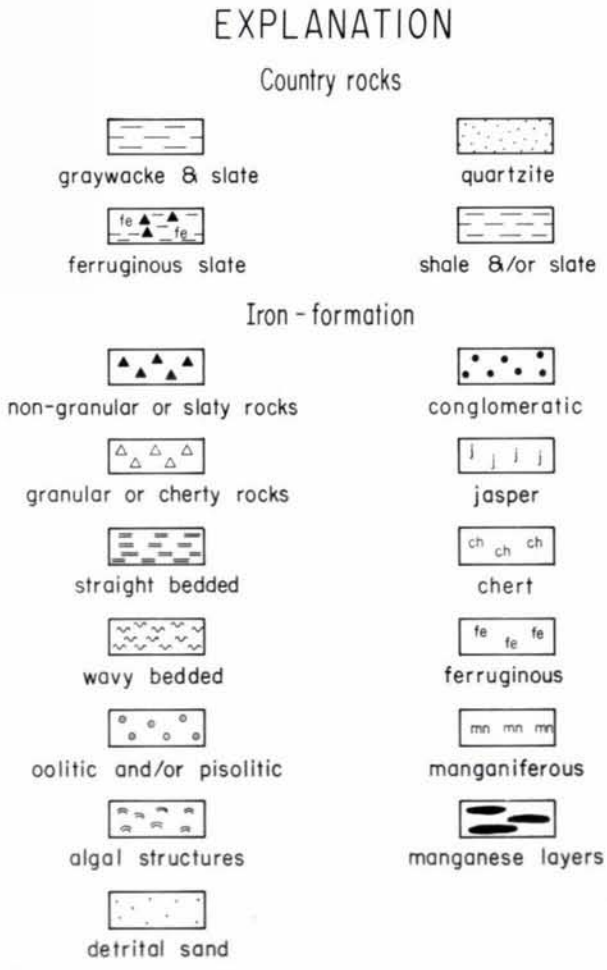

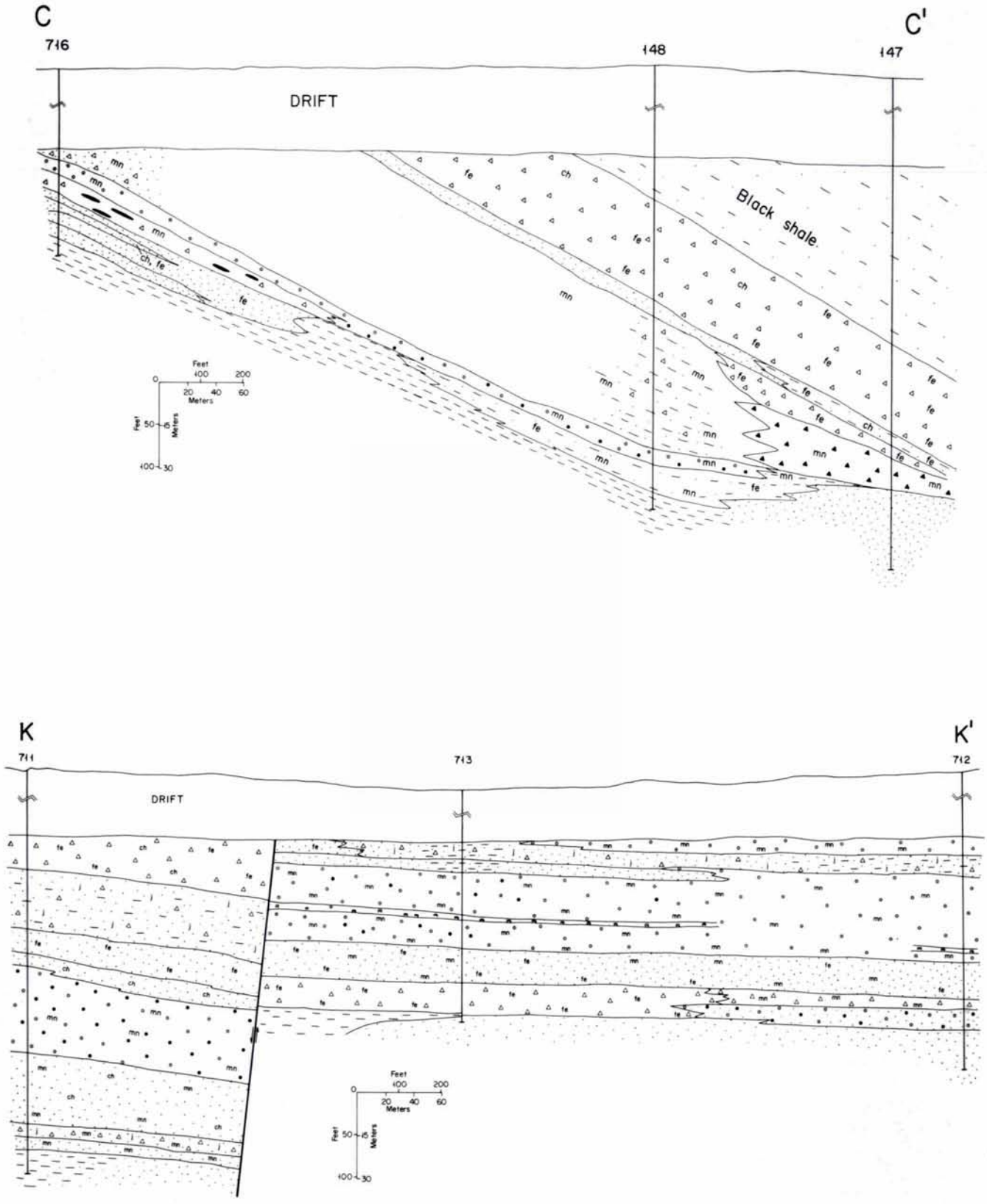

Figure 6. Continued

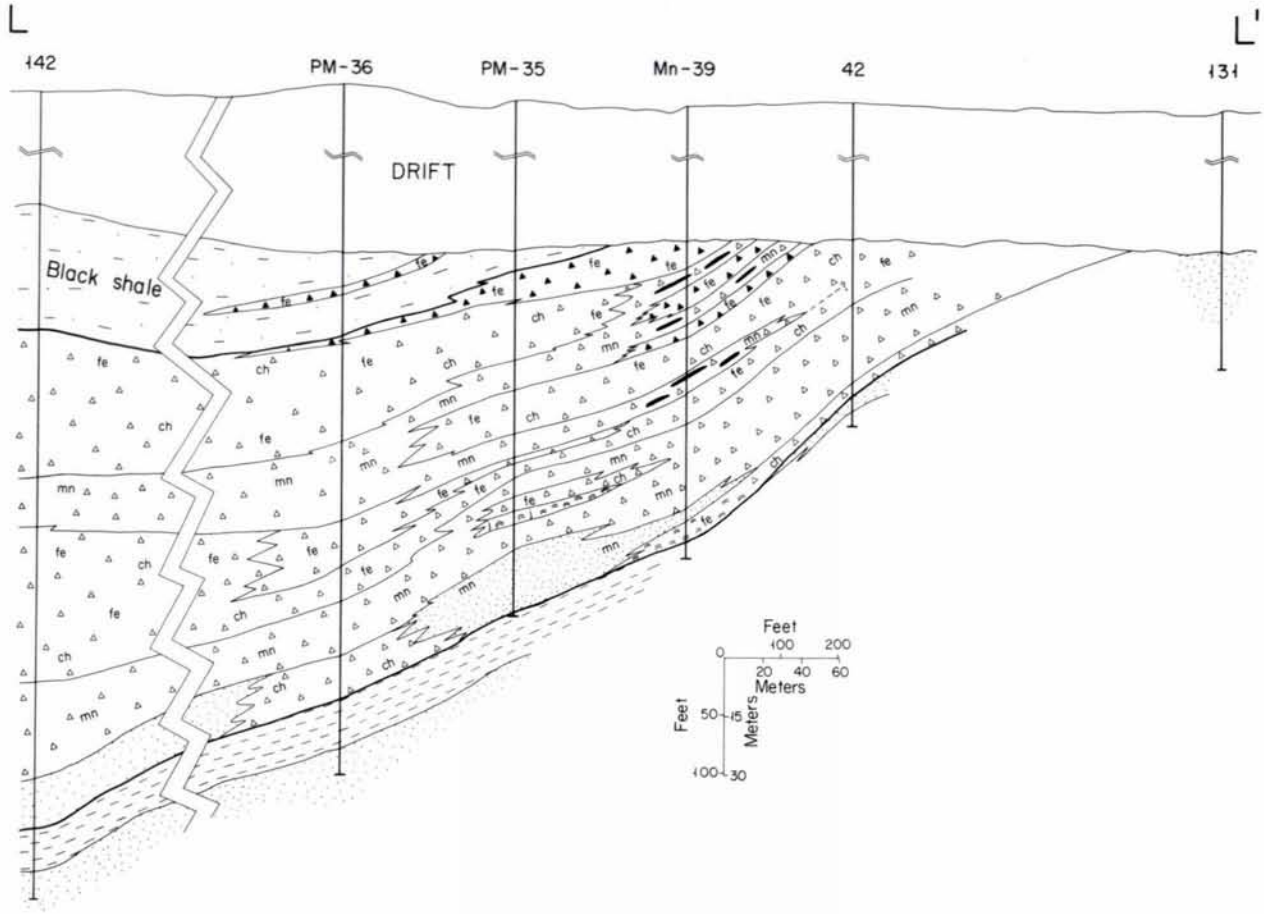

Figure 6. Continued

overlying black argillite through an interval of interbedding. Thus the upper contact of the ferruginous chert lithotope marks the end of the second cycle of chemical sedimentation in the Ruth Lake area. The lithotopes are broadly similar to the "facies" recognized by Marsden (1972), although he combined the algal and oolitic rocks into a single unit, whereas we find it useful to distinguish them. A brief description of each lithotope follows.

The iron-rich strata of the Ruth Lake area are chert-rich chemical sedimentary rocks that contain at least 15 percent iron (Fig. 8) and therefore are iron-formations by the criteria of James (1955). Moreover other chemical constituents such as P_2O_5 (Fig. 8) show distribution patterns characteristic of Precambrian iron-formations in general (Lepp and Goldich, 1964) and the Biwabik Iron Formation in particular (Lepp, 1966; Morey and Morey, 1990). However, Unit A at Ruth Lake is atypical in that much of it is neither thin bedded nor finely laminated—features also considered to be characteristic of iron-formations (James, 1955).

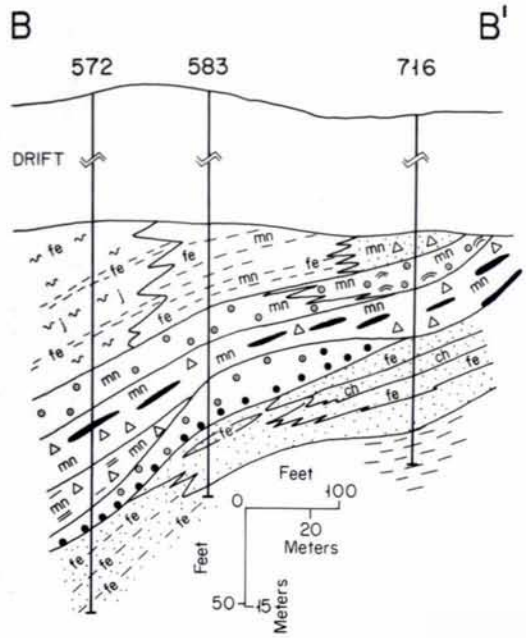

Figure 7. Selected cross sections showing the inferred distribution of lithotopes in Unit A at Ruth Lake. Locations of the sections are shown in Figure 5. Symbols are identified in Figure 6.

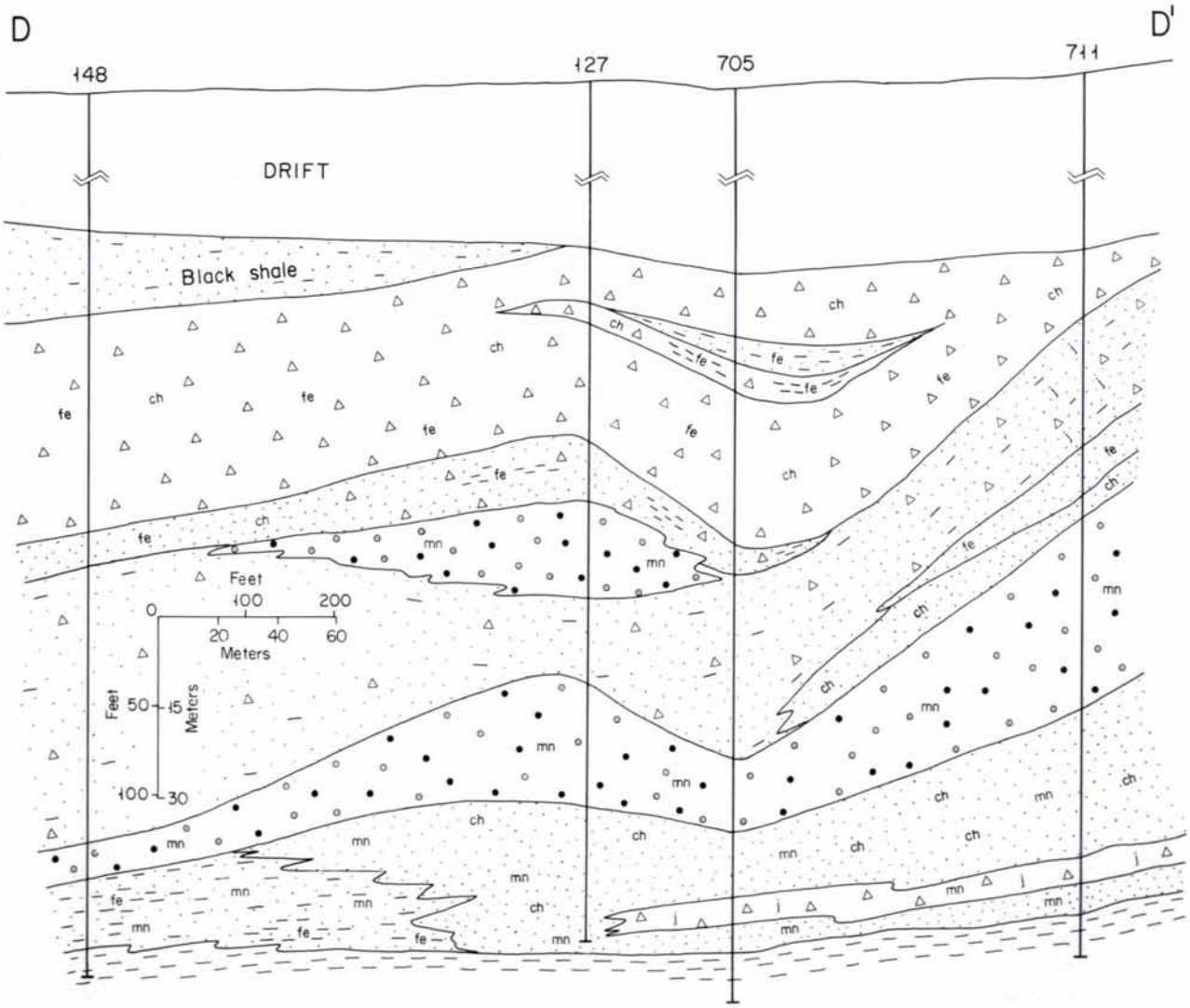

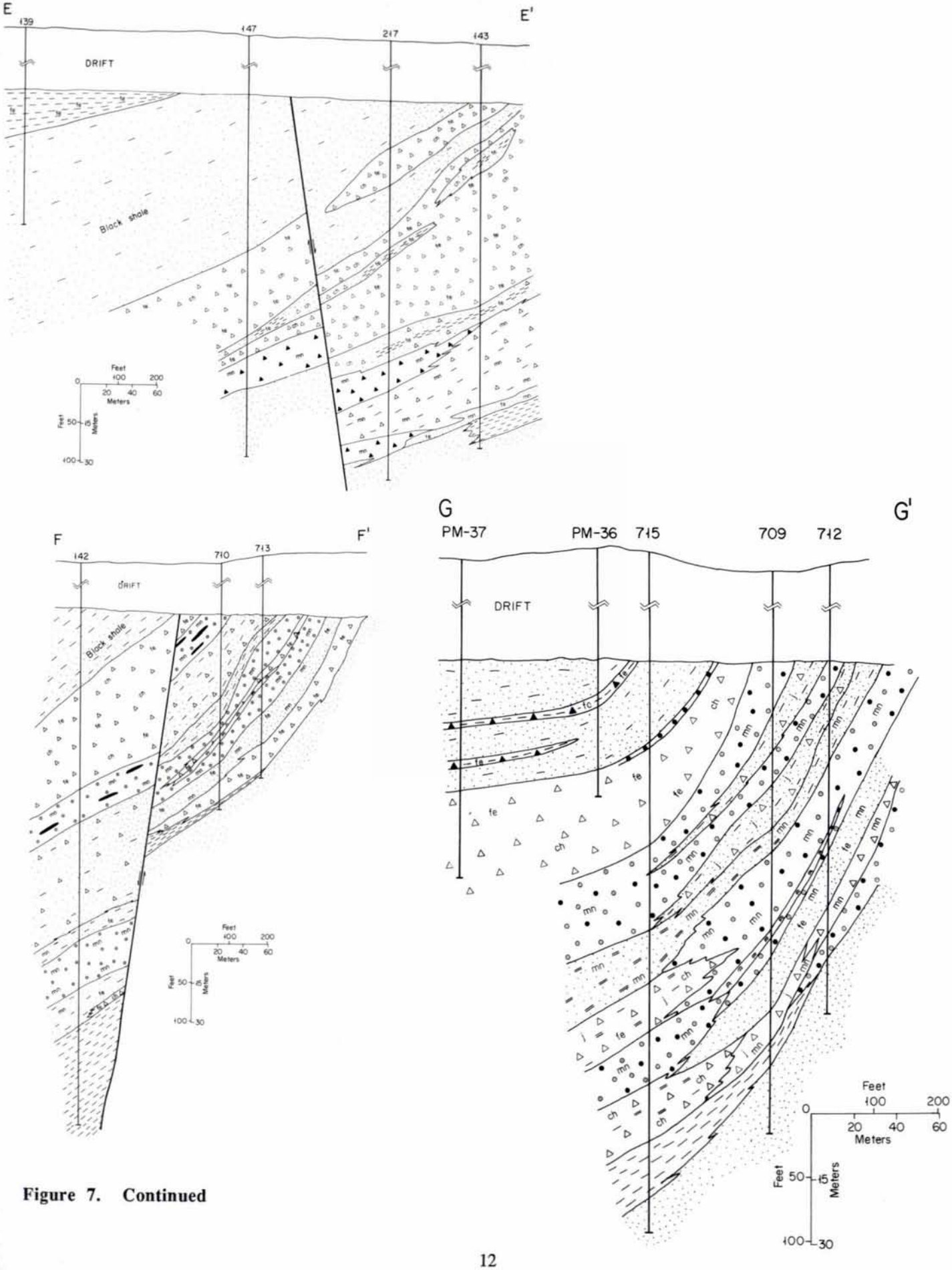

Figure 7. Continued

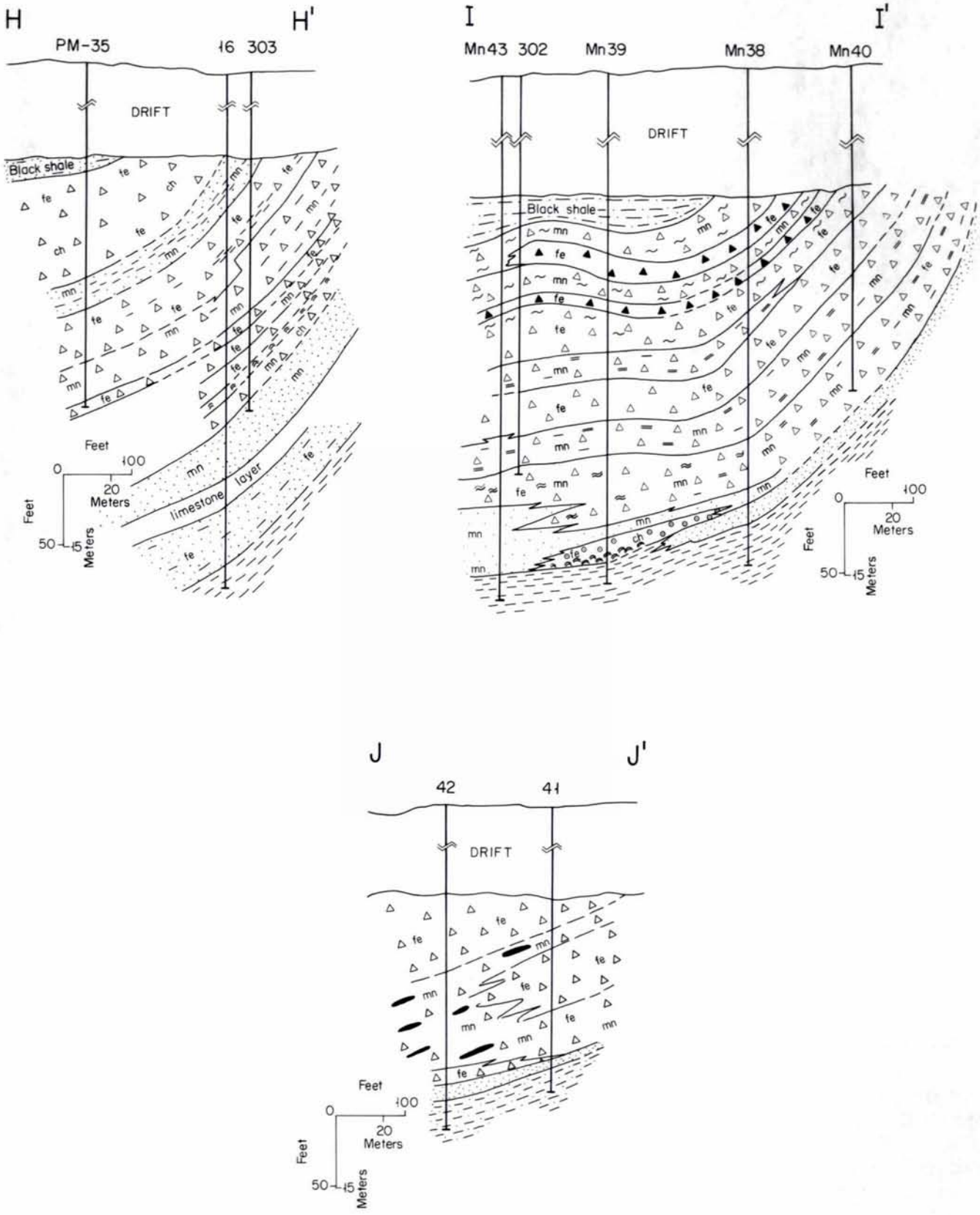

Figure 7. Continued

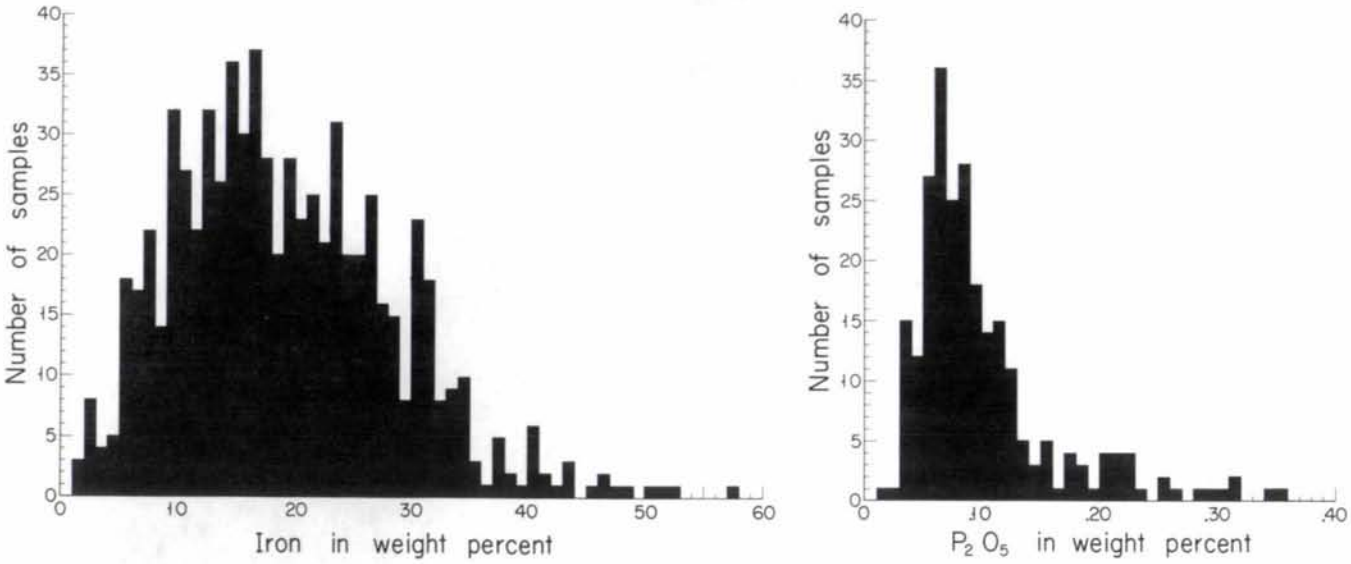

Figure 8. Histograms showing distribution of iron and P_2O_5 in 714 samples from Unit A of the Ruth Lake area.

Geochemistry and Mineralogy of the Lithotopes

The chemical analyses for most of the elements were performed by J.G. Kroening at the Geochemical Laboratories of the Department of Geology and Geophysics, University of Minnesota, Minneapolis. Values for Ag, As, Au, Hg, and Sb were determined by Geochemical Services, Inc., at Rocklin, California, by flame atomic absorption and X-ray fluorescence. The selected samples were from splits of AX core approximately 3 to 6 inches long.

The major elements do not sum to 100 percent in many samples, partly because the amount of material lost on ignition was not determined. We also chose to report the manganese values in the conventional way as MnO, even though the mineralogic evidence has clearly established that it occurs as MnO_2.

The mineralogy was determined by X-ray diffraction at the M.A. Hanna Research Center at Nashwauk, Minnesota, by Louis A. Mattson, analyst.

Lithotope 1 — Epiclastic Lithotope

The epiclastic lithotope in the Ruth Lake area consists predominantly of very thin to thin-bedded, quartz-rich siltstone and shale intercalated with intervals 1 to 3 meters thick of medium- to thick-bedded quartz arenite. Thus the lithotope is a continuation of the dominantly epiclastic sequence of rocks assigned to the Pokegama Quartzite.

Intervals of siltstone and shale are typically aluminous rocks (Table 1) characterized by beds and laminae that contain varying proportions of quartz and sericite; lesser amounts of minnesotaite and kaolinite or chamosite (Table 2) may also be present. These rocks contain dispersed medium-sand-size grains of quartz that are typically rounded to well rounded. Marsden (1972, p. 230) reports that some of the shaly beds, although nearly devoid of silt-size material, may contain as much as 30 modal percent sand-size grains.

Beds of medium- to coarse-grained quartz arenite occur at several stratigraphic levels in the lithotope. Most arenite beds are internally structureless, but a few appear to be vaguely content-graded and cross-bedded. The quartz arenite typically consists of rounded or subrounded sand-size grains of quartz and minor chert and jasper. Some quartz arenite units lack matrix material, whereas others are poorly sorted and are lithified by a matrix of silt-size quartz, sericite, and chamosite. Much of the matrix material occupies interstitial voids between touching framework grains, but in a few samples the framework component appears to float in the matrix. Some of the quartz arenitic units, regardless of texture, have lenses and/or clasts of chert and jasper. Beds of quartz arenite that lack appreciable matrix material in both the Pokegama Quartzite and the lower part of the epiclastic lithotope typically contain some interstitial calcite or siderite, but they are for the most part indurated by a silica cement. In contrast, similar beds toward the top of the lithotope are cemented by iron and manganese oxides (Table 2). Except for the presence of the manganese oxides, this lithotope markedly resembles the transition between the Pokegama Quartzite and the Biwabik Iron Formation on the north side of the Animikie basin, particularly in the central part of the Mesabi range.

Table 1. Chemical analyses of selected samples from the epiclastic lithotope

Values in weight percent except as noted

Sample no.	(1)	(2)	(3)	(4)	(5)
Hole no.	142	572	709	711	711
Depth (ft.)	675a	325	450	430	330
SiO_2	62.62	63.63	65.9	88.4	83.2
Al_2O_3	1.46	15.13	2.26	447+	4.66
TiO_2	572+	0.44	391+	24.3+	0.35
Fe_2O_3 Total	27.3	14.0	21.2	4.76	9.19
MnO	8.30	0.29	7.37	0.85	1.26
MgO	375+	1.15	0.12	554+	0.34
CaO	648+	518+	840+	115+	193+
Na_2O	552+	481+	451+	135+	266+
K_2O	0.27	5.15	0.11	401+	1.39
P_2O_5	711+	0.11	956+	300+	260+
CO_2	<.07	<.07	<.07	2.37	2.81
Sr	454+	63.0+	703+	16+	37.2+
Ba	.15	0.20	0.55	410+	0.34
		Values in ppm			
Hf	4.	8.	5.	6.	13.
Zr	37.	158.	42.	<3.	67.
Y	20.6	7.1	19.8	3.1	10.4
Be	2.08	3.75	1.63	.20	1.10
Zn	24.1	36.4	36.1	<1.8	11.2
Cu	1.9	3.5	22.5	2.7	1.7
Sc	<.3	8.1	1.0	<.5	4.1
Co	33.	22.	49.	<6.	18.
Pb	<37.	<39.	<60.	<56.	<73.
Ni	19.	42.	29.	4.	10.
Cr	4.	79.	<4.	<4.	12.
Rb	<96.	186.	<157.	<367.	<425.
V	85.	49.	<4.	7.	26.
Ag	<.015	<.015	<.015	<.015	<.015
As	10.5	15.4	45.9	3.63	3.96
Au	.002	.002	<.0005	.001	<.0005
Hg	.607	.393	.674	.148	.342
Sb	.327	<.242	<.246	<.246	<.25

+ indicates values in parts per million

1. 142-675a—Quartz arenite; rounded, medium sand-size grains of quartz and chert cemented by iron and manganese oxides.
2. 572-325—Slate, shale, or argillite; ferruginous; locally contains scattered, rounded, medium sand-size grains of quartz; intercalated with quartz arenite.
3. 709-450—Quartz arenite; ferruginous, cemented by or matrix replaced by iron and manganese oxides.
4. 711-430—Quartz arenite; medium to coarse sand-size grains of quartz cemented by iron and manganese oxides. Intercalated within an interval of stromatolite-bearing jasper. Note: An undissolved white precipitate formed as the sample was dissolved into solution during analysis.
5. 711-330—Quartz arenite; cemented by iron oxides or a ferruginous granular chert; intercalated with manganese-rich beds in the upper enriched zone.

Table 2. Mineralogy of selected samples from the epiclastic lithotope

Sample No.	(1)	(2)	(3)	(4)	(5)
Hole No.	142	142	709	711	709
Depth (ft.)	675a	675b	450	430	345a
Manganite	+	-	Tr	-	+
Pyrolusite	-	-	-	-	-
Psilomelane	-	-	-	-	-
Cryptomelane	-	-	Tr	-	-
Braunite	-	-	-	-	-
Hematite	+	+	+	+	+
Goethite	-	+	-	-	-
Quartz	++	++	++	++	++
Calcite	-	+	-	-	+
Siderite	-	-	-	-	+
10Å Mica	-	-	-	-	+
Kaolinite	-	+	+	-	-
Minnesotaite	-	-	+	+	-
Other	-	-	-	-	-

++, abundant; +, present; Tr, Trave; -, not observed

1. 142-675a—Quartz arenite; rounded, medium sand-size grains of quartz and chert cemented by iron and manganese oxides.
2. 142-675b—Quartz arenite; similar to sample 142-675a except for an obvious interstitial matrix of quartz and minnesotaite.
3. 709-450—Quartz arenite; rounded, fine to medium sand-size grains of quartz cemented by manganese and iron oxides; thick bedded with shaly and oolitic partings.
4. 711-430—Quartz arenite; medium to coarse sand-size grains of quartz cemented by silica and hematite. Intercalated within an interval of stromatolite-bearing jasper.
5. 709-345a—Quartz arenite; as above, exept cemented by a mixture of iron and manganese oxides.

Lithotope 2 — Mixed Epiclastic-Jaspery Chert Lithotope

This lithotope ranges from about 5 to 8 meters in thickness. It consists of beds of iron- and manganese-oxide-cemented quartz arenite intercalated with beds of jasper that are a meter or so thick. The jasper beds typically contain in situ stromatolitic structures, and the beds in turn are intercalated with beds of jasper-cemented conglomerate. Pebble-size clasts in the conglomeratic beds have an angular shape and consist either of broken stromatolitic materials or of jasper, identical in composition with that of the enclosing cement. The clasts obviously are locally derived and of intraformational origin.

All of the stromatolitic material is fine grained and composed of alternating laminae of gray chert and jasper. Where the structures are in place, the laminae form upwardly convex arches in columns that resemble stacks of thimbles.

Sand-size grains of terrigenous quartz are ubiquitous through the lithotope. Manganese oxides, mainly cryptomelane, also are ubiquitous constituents, occurring as disseminated grains in both the quartz arenite and conglomerate. In places, manganese oxides are so abundant that they form distinct lens-shaped masses. Some of the quartz arenite also contains small interstitial grains of siderite or ankerite. Consequently the chemical (Table 3) and mineralogical (Table 4) features of this lithotope can be attributed to a mixed epiclastic and chemically precipitated assemblage.

Except for the manganese mineralization, this lithotope strongly resembles the so-called "basal red taconite" found at the bottom of the Biwabik Iron Formation on the Mesabi range.

Table 3. Chemical analyses of selected samples from the mixed epiclastic-jaspery chert lithotope

Values in weight percent except as noted

Sample no.	(1)	(2)
Hole no.	127	217
Depth (ft.)	400b	580a
SiO_2	95.8	42.1
Al_2O_3	0.51	1.78
TiO_2	488+	732+
Fe_2O_3 Total	7.04	25.1
MnO	651+	21.8
MgO	0.40	665+
CaO	496+	.21
Na_2O	116+	707+
K_2O	54+	0.59
P_2O_5	521+	.19
CO_2	<.07	<.07
Sr	2.6+	553+
Ba	6.1+	.47
	Values in ppm	
Hf	9	<4.
Zr	10.	21
Y	12	15.4
Be	0.19	1.05
Zn	3.7	42.6
Cu	1.8	48.2
Sc	<.5	<.3
Co	7	88
Pb	<42	<36
Ni	3	12
Cr	4	11
Rb	<150	<94
V	76	40
Ag	.002	<.015
As	1.30	28.4
Au	.268	.001
Hg	2.53	.713
Sb	<.231	<.249

+ indicates values in parts per million

1. 127-400b—See Table 4 for sample description.
2. 217-580a—See Table 4 for sample description.

Table 4. Mineralogy of selected samples from the mixed epiclastic-jaspery chert lithotope

Sample No.	(1)	(2)	(3)	(4)
Hole No.	127	127	217	217
Depth (ft.)	400a	400b	580a	580b
Manganite	-	-	-	-
Pyrolusite	-	-	-	-
Psilomelane	-	-	-	-
Cryptomelane	-	Tr	++	+
Braunite	-	-	-	-
Hematite	+	+	+	++
Goethite	-	+	+	+
Quartz	++	++	++	++
Calcite	-	-	-	-
Siderite	-	-	-	+
10Å Mica	-	-	-	-
Kaolinite	-	-	-	+
Minnesotaite	-	-	-	+
Other	-	-	-	-

++, abundant; +, present; Tr, trace; -, not observed

1. 127-400a—Jasper with in situ stromatolitic units cemented by a cherty groundmass containing a few scattered sand-size grains of quartz.
2. 127-400b—Jasper, thin bedded with scattered rounded sand-size grains of quartz; cemented mainly by iron oxides and trace amounts of manganese oxides.
3. 217-580a—Composite sample consisting of jaspery chert intercalated with thicker manganese-rich layers or lenses apparently enclosed within manganese-oxide-cemented quartz arenite or manganese-rich granular iron-formation.
4. 271-580b—Iron-oxide-cemented quartz arenite with conglomeratic clasts of jasper and chert.

Table 5. Mineralogy of selected samples from the oolitic and pisolitic lithotope

Sample no.	(1)	(2)	(3)
Hole no.	572	709	709
Depth (ft.)	293	425a	425b
Manganite	-	-	Tr
Pyrolusite	+	-	Tr
Psilomelane	-	-	-
Cryptomelane	++	++	+
Braunite	-	-	-
Hematite	-	+	+
Goethite	+	+	+
Quartz	+	+	Tr
Calcite	-	-	-
Siderite	-	-	-
10Å Mica	-	-	-
Kaolinite	-	-	-
Minnesotaite	+	+	-
Other	-	-	-

++, abundant; +, present; Tr, trace; -, not observed

1. 572-293—Iron- and manganese-bearing oolites set in a matrix of granular chert and disseminated iron oxides.
2. 709-425a—Manganese-rich oolites set in a matrix of granular chert and disseminated iron oxides.
3. 709-425b—Massive iron and manganese oxide-rich unit intercalated with sample 709-425a.

Lithotope 3 — Oolitic and Pisolitic Lithotope

The oolitic and pisolitic lithotope forms stratigraphic units as much as 18 meters thick in the Ruth Lake area. As the name implies, this lithotope consists predominantly of oolitic and pisolitic structures, some of which are as much as 7 cm in diameter. The pisolites, as well as the much smaller oolites, have rims of manganese oxides that surround alternating shells of quartz and either hematite or goethite around core grains of terrigenous quartz. Similar quartz grains that lack rim material also occur randomly scattered throughout the lithotope. These framework grains and structures are cemented in places by goethite but more commonly by mixtures of the manganese oxides, especially cryptomelane and pyrolusite (Table 5). The lithotope also contains thin to thick beds composed predominantly of manganese oxides mosaically intergrown with various amounts of goethite and quartz. Nodules or lenses of chert and jasper also occur at several places in the lithotope. Because this lithotope has diverse textural and mineralogical attributes, its chemical characteristics (Table 6) vary widely, even over stratigraphic intervals of only a few centimeters.

The oolitic and pisolitic lithotope has no significant counterpart in the Biwabik Iron Formation of the Mesabi range.

Table 6. Chemical analyses of selected samples from the oolitic and pisolitic lithotope

Values in weight percent except as noted

Sample no.	(1)	(2)
Hole no	572	709
Depth (ft.)	293	425a
SiO_2	57.4	23.0
Al_2O_3	0.88	1.01
TiO_2	176+	0.10
Fe_2O_3 Total	23.3	36.7
MnO	12.2	28.0
MgO	0.17	0.10
CaO	0.17	0.19
Na_2O	754+	0.25
K_2O	0.50	2.36
P_2O_5	0.16	0.22
CO_2	<.07	<.07
Sr	780+	0.203
Ba	0.65	0.25
	Values in ppm	
Hf	5	<4
Zr	17.7	35
Y	32.1	53.7
Be	2.62	3.65
Zn	37.8	37.9
Cu	7.8	18.1
Sc	<.3	0.6
Co	43	63
Pb	<50	<61
Ni	26	33
Cr	<4	<4
Rb	<131	<147
V	16	19
Ag	<.015	<.015
As	123.	107.
Au	<.0005	<.0005
Hg	1.95	.664
Sb	.614	.597

+ indicates values in parts per million

1. 572-293—Iron- and manganese-bearing oolites set in a matrix of granular chert and disseminated iron oxides.
2. 709-425a—Manganese-rich oolites set in a matrix of granular chert and disseminated iron oxides.

Lithotope 4 — Thick-bedded Lithotope

The thick-bedded lithotope occurs as stratigraphic intervals as much as 11 to 13 meters thick. It consists for the most part of beds of so-called "granular" or "cherty" iron-formation. These strata are characterized by ovoid granules, generally about 1 mm in diameter, of chert, hematite, or goethite, or mixtures of these minerals set in a groundmass of coarse-grained white or gray chert. Disseminated grains of iron and manganese oxides also occur in the cherty groundmass as do scattered patchy concentrations of goethite about 2 cm in diameter. These so-called "mottles" are clearly of secondary origin. They have irregular gradational boundaries and seem to include chert and hematite, but not the manganese oxides. The lithotope also contains scattered and generally thin intervals of regularly bedded or irregularly to wavy-bedded layers composed predominantly of iron oxides. The regularly bedded layers, as much as 7 cm thick, are relatively straight and more or less parallel to primary layering. Contacts with enclosing strata may be sharp or gradational over 0.3 cm or so. The irregularly or wavy-bedded layers typically swell and pinch, split and reunite, and connect with adjacent layers. They range in thickness from wisps or very thin laminae to beds 5 to 7 cm thick and commonly have sharp boundaries.

Table 7. Mineralogy of selected samples from the thick-bedded and mixed thick- and thin-bedded lithotopes

Sample no.	(1)	(2)	(3)	(4)	(5)	(6)	(7)	(8)	(9)	(10)
Hole no.	217	217	709	711	711	572	709	709	572	709
Depth (ft.)	580a	580b	340	315	330	325	357a	357b	247	345b
Manganite	+	+	+	+	+	-	-	-	+	+
Pyrolusite	-	-	-	-	-	-	-	-	Tr	-
Psilomelane	-	-	-	-	-	-	-	-	-	+
Cryptomelane	++	+	Tr	-	-	-	+	+	+	-
Braunite	-	-	-	-	-	-	-	-	-	-
Hematite	+	++	++	+	+	+	+	-	+	+
Goethite	+	+	Tr	-	-	-	+	+	+	-
Quartz	++	Tr	++	++	++	++	++	-	++	++
Calcite	-	-	+	-	-	-	-	-	-	-
Siderite	-	-	-	-	-	-	Tr	-	-	-
10Å Mica	-	-	+	+	+	++	-	-	-	+
Kaolinite	-	-	-	+	+	+	-	-	-	+
Minnesotaite	+	-	-	-	-	++	++	-	-	-
Other (Chlorite)	-	-	-	-	+	-	-	-	-	-

++, abundant; +, present; Tr, trace; -, not observed

1. 217-580a—Iron-formation, granular, with disseminated grains and granules of iron oxides.
2. 217-580b—Iron-oxide-rich layers with scattered iron-oxide granules and massive interlocking grains of manganese oxides.
3. 709-340—Iron-formation, granular, with disseminated grains of iron and manganese oxides; interlayered with thin beds of massive manganese oxides.
4. 711-315—Iron-formation, granular, somewhat oxidized and leached, with disseminated grains of hematite and thin laminae of kaolinite and sericite.
5. 711-330—Iron-formation, non-granular, thin bedded, interlayered with laminae of granular iron-formation with disseminated manganese oxides.
6. 572-325—Iron-formation, non-granular, thin bedded, somewhat soft and earthy.
7. 709-357a—Iron-formation, non-granular, thin bedded; intercalated with manganese-oxide-rich layers.
8. 709-357b—Iron-formation, non-granular; manganese-oxide-rich layer interbedded with sample 709-357a..
9. 572-247—Iron-formation, granular, with disseminated manganese oxides, scattered oolites, and rounded quartz grains.
10. 709-345b—Iron-formation, granular, with disseminated manganese oxides.

As with the other lithotopes, sand-size grains of terrigenous quartz are scattered throughout. The lithotope also contains several manganese oxides, including appreciable quantities of manganite as disseminated grains in the granular layers. Manganite also occurs as thin, sharply bounded monomineralic layers within granular intervals, and together with cryptomelane, it forms thin to thick, regularly and irregularly bedded layers or lenses, both with and without iron oxides.

The textural features of the thick-bedded lithotope are identical in all respects to those observed in cherty or granular strata of the Biwabik Iron Formation of the Mesabi range. There, however, ferrous iron is abundant and the oxide phase is primarily magnetite, whereas here in Unit A the iron oxide phases are predominantly hematite and goethite (Table 7). Nonetheless, the chemical attributes of this lithotope (Table 8), except for manganese, are broadly similar to those of cherty strata in the Biwabik Iron Formation (e.g., Morey and Morey, 1990).

Lithotope 5 — Mixed Thick- and Thin-bedded Lithotope

The mixed thick- and thin-bedded lithotope can be as much as 13 meters thick in Unit A. It is texturally and mineralogically identical with the thick-bedded lithotope and is distinguished from it only by the presence of thick layers of so-called "non-granular" or "slaty" iron-formation. These slaty intervals are typically very thin bedded to laminated and are seemingly fine grained because they lack granules and coarse interstitial chert. However like the cherty or granular rocks, they contain appreciable quartz and goethite (Tables 7 and 9). The slaty rocks also contain minnesotaite, a 10A mica (most likely sericite), and kaolinite—silicate minerals not typically associated with granular strata in Unit A.

Manganese oxides occur only very sparingly in the slaty intervals in this lithotope. However they can be found as disseminated grains in cherty beds. In places the manganese oxides form thin to thick beds that are mosaically intergrown with iron oxides.

Table 8. Chemical analyses of selected samples from the thick-bedded and mixed thick- and thin-bedded lithotopes

Values in weight percent except as noted

Sample no.	(1)	(2)	(3)	(4)
Hole no.	572	709	711	709
Depth (ft.)	247	357a	379	345
SiO_2	68.6	33.20	25.5	70.1
Al_2O_3	0.45	3.03	4.29	0.65
TiO_2	127+	0.24	0.18	368+
Fe_2O_3 Total	15.3	32.8	41.0	29.9
MnO	9.90	18.90	16.22	1.30
MgO	642+	0.27	2.02	491+
CaO	802+	0.260	1.60	0.15
Na_2O	422+	0.39	1.34	167+
K_2O	0.18	1.99	3.27	0.11
P_2O_5	899+	0.38	0.16	543+
CO_2	<.07	<.07	0.09	<.07
Sr	113+	0.17	0.10	19.3+
Ba	.38	0.20	0.81	554+
	Values in ppm			
Hf	8	6	8	8
Zr	14	163	72	14
Y	19.4	58.3	20.5	6.7
Be	1.12	3.22	1.7	.92
Zn	17.2	15.7	46	<2
Cu	14.8	109.3	53.8	1.0
Sc	<.4	3.8	3.1	<.4
Co	22	73	91	<5
Pb	<52	<32	250	<32
Ni	12	158	25	<2.1
Cr	5	8	33	9.0
Rb	<146	<192	<423	<208
V	14	27	20	32
Ag	<.015	<.149	<.014	<.014
As	69.8	152.	113.	9.31
Au	<.0005	<.0005	<.0005	.001
Hg	.463	<.99	.664	1.14
Sb	.326	<2.47	.524	.333

+ indicates values in parts per million

1. 572-247—Iron-formation, granular or thick bedded with disseminated manganese oxides, scattered oolites and rounded quartz grains.
2. 709-357a—Iron-formation, non-granular or thin bedded; intercalated with thick manganese oxide-rich layers.
3. 711-379—Iron-formation, non-granular or thin bedded, silicate rich; intercalated with thick intervals of massive manganese oxides.
4. 709-345b—Iron-formation, granular or thick bedded with disseminated manganese oxides.

Lithotope 6 — Ferruginous Chert Lithotope

The ferruginous chert lithotope is a special kind of slaty iron-formation. This lithotope, which in places is as much as 40 meters thick, is composed entirely of thin-bedded to laminated jasper and chert. Individual laminae are largely chert and hematite in various proportions; in places they include some siderite and minnesotaite (Table 9). In general, the lithotope lacks appreciable quantities of manganese (Table 10), although discrete layers or lenses of cryptomelane, generally less than 5 cm thick, occur within the lithotope near its lower contact.

The ferruginous chert lithotope passes transitionally upward into a thin-bedded sequence of black shale and siltstone that contains scattered lenses and layers of ferruginous chert. Bedding planes between the ferruginous chert and layers of shale or siltstone are regular and sharply defined, implying that epiclastic and chemical sedimentary events were separate and discrete.

Table 9. Mineralogy of selected samples from the ferruginous chert lithotope

Sample no.	(1)	(2)	(3)	(4)	(5)	(6)
Hole no.	127	127	142	142	143	147
Depth (ft.)	325a	325b	370a	370b	307	200
Manganite	-	-	-	-	-	Tr
Pyrolusite	-	-	-	-	-	-
Psilomelane	-	-	-	-	-	-
Cryptomelane	-	-	-	-	-	+
Braunite	-	-	-	-	-	-
Hematite	+	+	+	-	-	-
Goethite	-	-	+	+	+	+
Quartz	++	++	++	++	++	++
Calcite	-	-	-	-	-	-
Siderite	-	+	-	-	+	-
10Å Mica	-	+	-	-	-	++
Kaolinite	-	-	-	-	-	+
Minnesotaite	-	-	-	-	-	-
Other	-	-	-	-	-	-

++, abundant; +, present; Tr, trace; -, not observed

1. 127-325a—Ferruginous chert, somewhat oxidized; interlayered with sample 127-325b.
2. 127-325b—Ferruginous chert, somewhat oxidized and leached; interlayered with sample 127-325a.
3. 142-370a—Ferruginous chert; laminated chert and jasper.
4. 142-370b—Ferruginous chert; laminated chert, chert and silicates, and jasper or hematite.
5. 143-307—Carbonate-rich layer; somewhat oxidized.
6. 147-200—Silicate-rich layer; somewhat oxidized.

Table 10. Chemical analyses of selected samples from the ferruginous chert lithotope

Values in weight percent except as noted

Sample no	(1)	(2)	(3)
Hole no.	127	127	709
Depth (ft.)	325a	325b	340
SiO_2	51.2	40.7	40.
Al_2O_3	0.49	2.18	1.61
TiO_2	376+	846+	0.11
Fe_2O_3 Total	46.9	54.6	54.2
MnO	.20	0.401	2.60
MgO	813	0.21	914+
CaO	230+	261+	336+
Na_2O	212+	272+	266+
K_2O	0.17	0.83	0.13
P_2O_5	416+	408+	460+
CO_2	<.07	<.07	<.07
Sr	10.7+	14.4+	57.4+
Ba	98.6+	456+	0.37
	Values in ppm		
Hf	6	8	9
Zr	29	60	28
Y	20	34.9	14.5
Be	1.84	3.86	1.20
Zn	<1.8	<1.8	<2.
Cu	3.5	26.3	1.3
Sc	<.3	<.3	<3
Co	7	21	15
Pb	<38	<38	<33
Ni	19	11	20
Cr	4	27	13
Rb	<119	<119	<217
V	58	54	55
Ag	<.015	<.014	<.014
As	20.9	17.6	14.9
Au	.001	.009	.001
Hg	1.16	1.78	1.83
Sb	<.244	.669	.502

+ indicates values in parts per million

1. 127-325a—Ferruginous chert, somewhat oxidized; interlayered with sample 127-325b.
2. 127-325b—Ferruginous chert, somewhat oxidized and leached; interlayered with sample 127-325a.
3. 709-340—Ferruginous chert; oxidized and leached, intercalated with thin beds of manganese-oxide-cemented granular chert.

A SEDIMENTOLOGICAL MODEL

The general arrangement of lithotopes in Unit A of the Ruth Lake area implies a gradual change over time from predominantly epiclastic sedimentation in shallow water, through a period of predominantly chemical precipitation of silica and iron, to a second period of epiclastic sedimentation in deeper water (Fig. 9). This broad trend from shallower to deeper water deposition can in turn be divided into two subcycles in the time sequence such that the pattern shallower water → deeper water → shallower water → deeper water lithotopes is broadly similar to that observed in the Biwabik Iron Formation on the Mesabi range. There the pattern Lower cherty member (shallower), Lower slaty member (deeper), Upper cherty member (shallower), Upper slaty member (deeper) has been recognized for more than 70 years.

Physical Sedimentary Processes

White (1954) suggested for the Biwabik Iron Formation that thick-bedded and cherty or granular sediments were deposited in a shallow-water, agitated environment, and that slaty or thin-bedded, non-granular sediments were deposited in deeper, less active water. The vertical repetition of intercalated units of cherty and slaty iron-formation is suggestive of a depositional environment near an alternately transgressing and regressing strandline. Although White (1954) had a set of observations consistent with a moving strandline, he did not have a mechanism that could explain why the strandline moved. Goodwin (1956) emphasized the importance of volcanic materials in the Gunflint Iron Formation in Ontario and suggested that intercalated cherty and slaty materials there were related to the epiclastic tectonism. In this view, the floor of the depositional basin sloped more or less uniformly away from a strandline during periods of crustal stability. During episodes of crustal instability, however, the basin floor subsided, and the shallow-water units then were covered by deeper water materials which gradually filled the basin and eventually restored shallow-water conditions.

The idea of periodic crustal instability is central to the foredeep interpretation of the Animikie basin proposed by Hoffman (1987) and Southwick and others (1988). The foredeep units lapped onto the northern and northwestern cratonic foreland in response to tectonic loading in the hinterland to the south and southeast. Because tectonic processes tend to be episodic rather than continuous over time, the model predicts that the sedimentary responses on the cratonic basin margin also should be episodic.

In the Ruth Lake area, the ubiquitous sand-size grains of terrigenous quartz in the epiclastic, mixed epiclastic-jaspery chert, and oolitic-pisolitic lithotopes imply that deposition was near a strandline. Abrupt changes in these lithotopes in

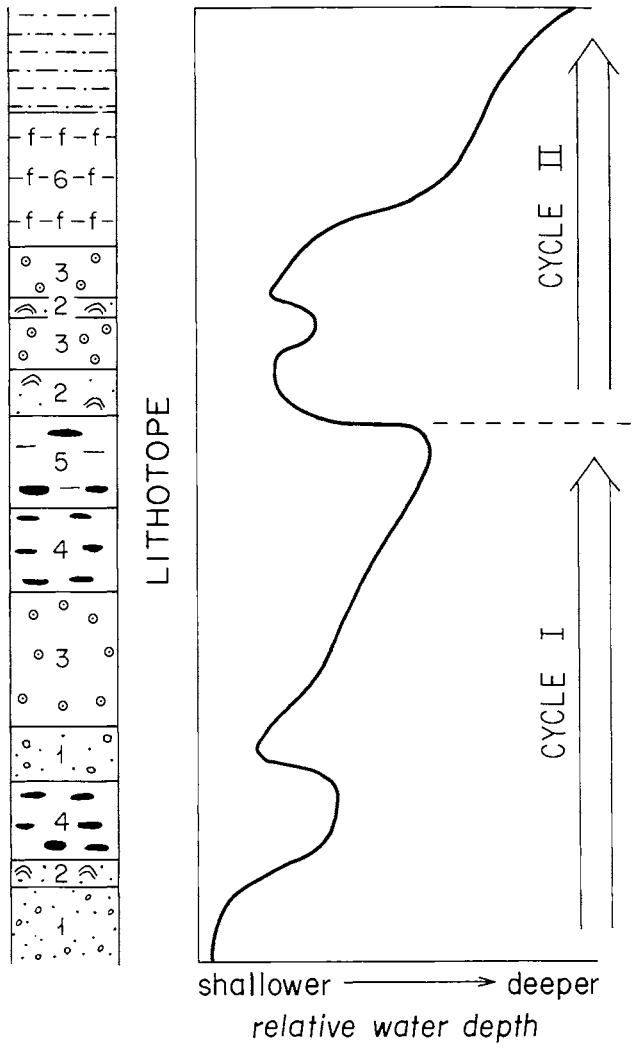

Figure 9. Diagram showing generalized upward-deepening attributes of Unit A strata in the Ruth Lake area inferred from cross section G-G' in Figure 7. The terms "shallower" and "deeper" are relative and no vertical scale or absolute depths are intended. Note that each of the two cycles consists of two discrete "shallower" to "deeper" cycles.

the down-dip direction (Fig. 6) combined with their lateral persistence in the strike-parallel direction (Fig. 7) imply that the depositional basin deepened toward the north. The inferred stratigraphic relationships are illustrated in Figure 10. The location of thick-bedded iron-formation in this depositional reconstruction is somewhat uncertain, but the lithotope seems to be better developed in the southern or up-dip parts of the section. Similarly, thin-bedded iron-formation in the mixed lithotope seems to be more abundant in the northern or down-dip parts of the section. This arrangement implies that the thick-bedded and the mixed thick- and thin-bedded lithotopes were deposited under generally similar sedimentological conditions, but that the latter was deposited in a slightly less agitated, perhaps deeper, environment. The position of the ferruginous chert lithotope in this reconstruction also is problematic. However, because it is everywhere overlain by and in places interbedded with clastic rocks having "deeper water" affinities (Morey, 1983), it most likely accumulated under very quiet conditions in water presumably deeper than that responsible for the other lithotopes.

The reconstruction in Figure 10 is broadly analogous in stratigraphy, structure, and texture to pretidal-platform/carbonate-ramp/shale-filled-basin sequences in rocks of Phanerozoic age. Phanerozoic depositional sequences of this kind reflect transition from a shaly or limy mudstone facies (open water) through oolitic limestone facies (shoal) to admixed facies of organic, fine-grained clastic, and chemical sediments (back-shoal platform). In the Ruth Lake area, a storm wavebase (where waves first impinge upon the bottom) is marked by the appearance of discrete grainy beds (lithotope 4). The grainy units pass offshore into muddier beds (lithotopes 5 and 6) and onshore into oolitic and pisolitic shoal deposits (lithotope 3) that also contain lenses and layers of conglomeratic material. The shoal rocks in turn pass shoreward into a back-ramp platform sequence characterized by cyclic shallow to supratidal deposits (lithotopes 1 and 2). Thus it can be concluded that the Ruth Lake strata were deposited on a shelf in a physical sedimentological regime that was not much different from that of a modern shelf.

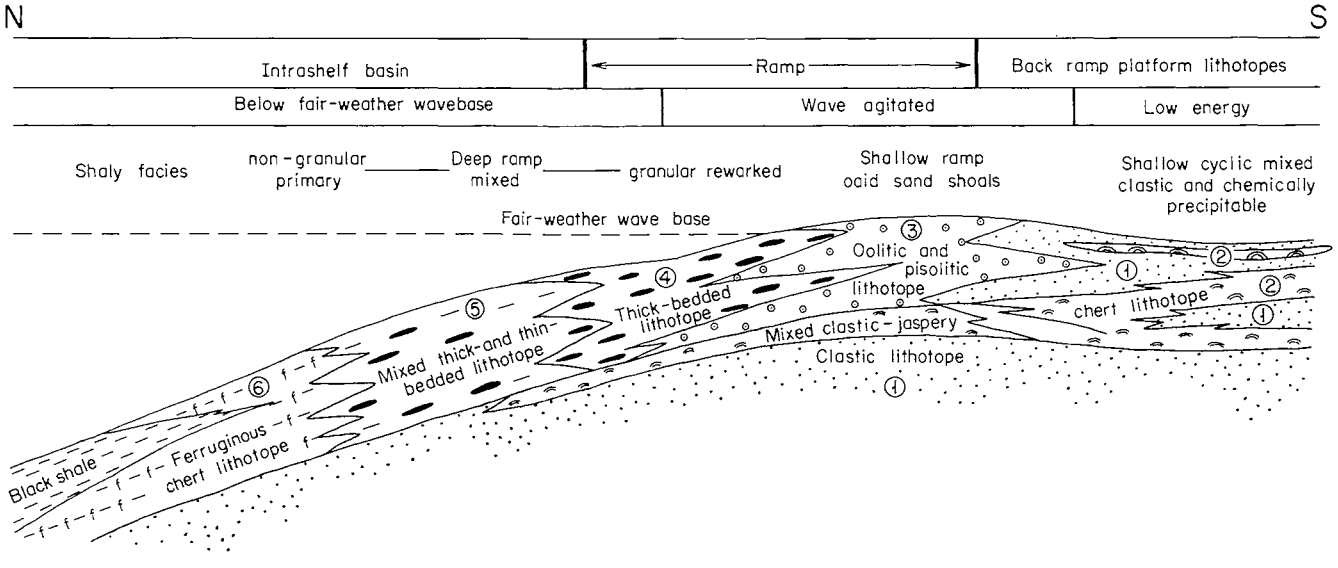

Figure 10. Schematic profile of lithotopes in the Ruth Lake area as inferred from vertical relationships in Figure 9. No vertical or horizontal scale intended. Environmental nomenclature modified from Markello and Reed (1981).

Chemical Sedimentary Processes

Unit A at Ruth Lake consists predominantly of chemically precipitated chert, iron oxides, and manganese oxides; appreciable terrigenous quartz; and minor amounts of minnesotaite, sericite, chamosite, and chlorite—minerals that may be either detrital or epigenetic. There is no direct evidence, however, that any of the minerals we observe today, other than detrital quartz, are those originally deposited. Nonetheless, the bulk chemical composition of Unit A can be approximated by the four constituents SiO_2, Al_2O_3, and Fe_2O_3 + MnO (Fig. 11). These four constituents typically make up more than 85 percent and, in some samples, as much as 99 percent of the Ruth Lake sequence.

In Figure 11, where SiO_2, Al_2O_3 and Fe_2O_3 + MnO values have been recalculated to 100 percent, most of the chemically precipitated iron-rich rocks, regardless of textural attributes, have SiO_2 values of less than 55-60 percent. Samples with silica values of 60 percent or more define a second group that is also characterized by somewhat elevated alumina values which reflect the presence of a shaly or silty component not easily seen in hand specimens. Although Unit A is compositionally similar to the magnetite-bearing rocks of the Biwabik Iron Formation (Morey and Morey, 1990), it contains more alumina (on the average generally >1%), an attribute that most likely reflects the presence of a terrigenous component at Ruth Lake not present on the Mesabi range. The broad similarity of compositional attributes of both iron-rich sequences implies that both were derived from a well-mixed chemical reservoir that apparently changed little in composition over time (Lepp, 1987).

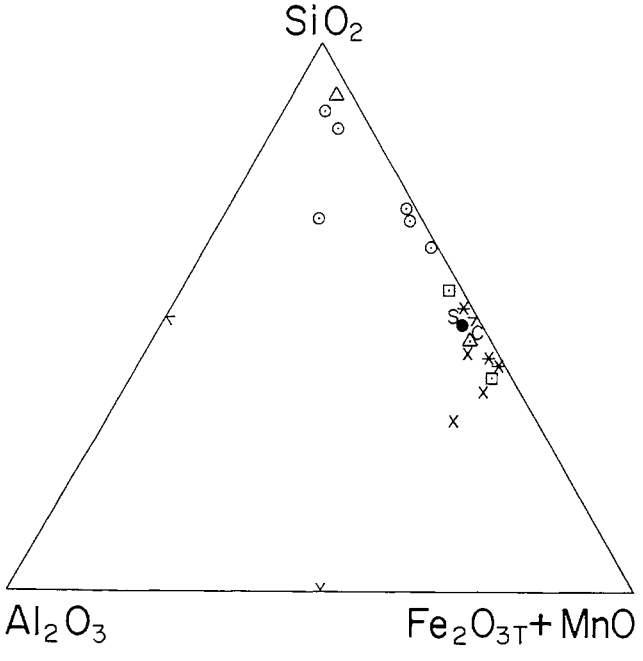

Figure 11. Silica—alumina—total iron and manganese oxide plot of various lithotopes in Unit A as compared to the Biwabik Iron Formation. ⊙, lithotope 1; △, lithotope 2; ⊡, lithotope 3; ×, lithotopes 4 and 5; ✳, lithotope 6; •, average Biwabik composition; S, average for slaty rocks in the Biwabik; C, average for cherty rocks in the Biwabik.

The two iron-rich sequences differ considerably in mineralogical attributes. In particular, magnetite and other minerals that contain a ferrous iron component are minor or lacking at Ruth Lake. The dominance of ferric over ferrous iron in Unit A has been ascribed to pervasive chemical weathering in late Mesozoic time (Marsden, 1972), but might also be due to syngenetic processes. It is generally accepted today that Precambrian iron-formations formed by processes broadly similar to those illustrated in Figure 12. Silica and ferrous iron from both anoxic weathering and volcanic sources accumulate in an extensive anaerobic marine basin. Upwelling of water rich in silica and iron from such a basin onto a shallow-water shelf leads to three separate but interrelated processes. First, the waters are warmed and carbon dioxide is lost, triggering the precipitation of siderite ($FeCO_3$). Second, nutrients in the upwelling waters stimulate the growth of algae and cyanobacteria and consequently the production of photosynthetic oxygen. The presence of that oxygen leads to the conversion of ferrous iron to ferric iron, the precipitation of insoluble ferric hydroxides, and their subsequent conversion to hematite. Unlike siderite and hematite, which are syngenetic minerals, magnetite produced in this setting is the diagenetic result of the reaction hematite + organic carbon → magnetite + carbon dioxide. This reaction shows that the amount of magnetite that can form is controlled by the amount of organic carbon available in the diagenetic system. The amount of available carbon would have been controlled in turn by the organic productivity of the photosynthetic zone and the extent to which dead organisms were oxidized and destroyed, or were reduced and preserved in the near-bottom environment. Consequently the lack of magnetite, siderite, or other ferrous minerals in the Ruth Lake area could be taken to mean (1) that precipitation occurred well within the photosynthetic zone and (2) that oxygen was sufficiently abundant in the photosynthetic zone to destroy organic material before it could accumulate in the diagenetic environment.

Lastly, it is generally held that organisms capable of building silica into their internal skeletons did not exist in

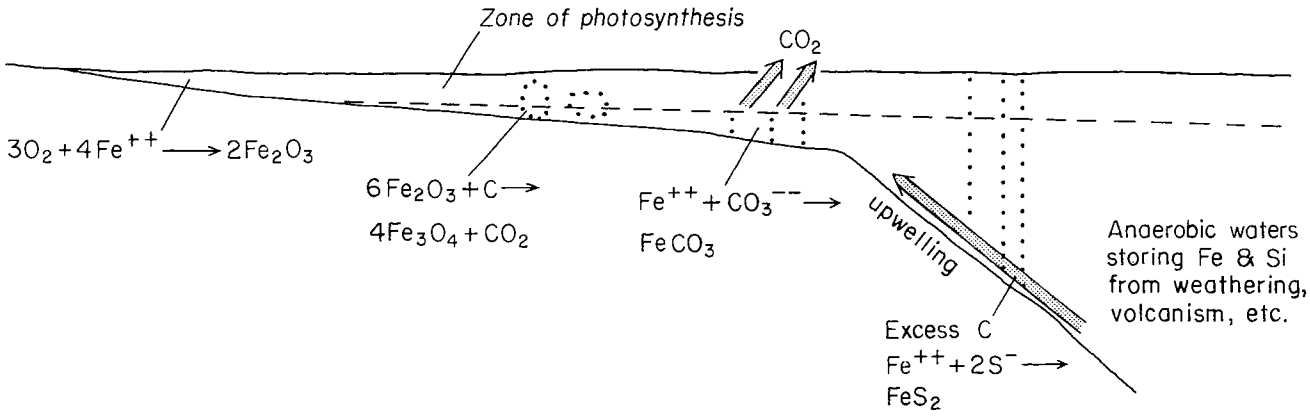

Figure 12. Schematic diagram showing the relationships between the precipitation of various iron-bearing minerals and subsequent diagenetic modifications relative to the amount of organic carbon in the depositional system.

Early Proterozoic time. Consequently the amount of silica in any given solution was controlled by the solubility of either amorphous silica or a hydrous silicate such as magadiite or greenalite (Ewers, 1983). The work of Krauskopf (1956) and Siever (1962), as well as others summarized by Walter and others (1972), shows that under these conditions the solubility of silica is favored in cold, alkaline solutions. Thus silica will precipitate in response to warming on a shallow-water shelf, a process that is enhanced when warming causes evaporation to occur (Eugster and Chou, 1973). Probably more important to the precipitation of silica, however, is the observation that the precipitation of iron, whether by oxidation of the ferrous to the ferric species and subsequent hydrolysis to a ferric oxide, or by forming carbonates or silicates, constitutes a release of acid and a trend toward a solution that is neutral to slightly alkaline, a condition that also favors the precipitation of silica.

In summary, both the physical and chemical sedimentological features of the iron-rich strata at Ruth Lake can be attributed to a shallow-water shelf environment where oxic conditions prevailed because of extensive photosynthetic activity by algae and cyanobacteria.

DISTRIBUTION OF MANGANESE-BEARING MATERIALS

In strong contrast to the Biwabik Iron Formation of the Mesabi range, Unit A in the Ruth Lake area contains a substantial amount of manganese. With a cutoff grade of 1 weight percent manganese averaged over a sample interval of 1.5 meters (5 feet), the data in Figures 13 and 14 show that the lower stratigraphic limit of anomalously high manganese occurs in the upper coarse-grained meter or so of the epiclastic lithotope, and the upper limit is effectively at the base of the ferruginous chert lithotope. Thus in a stratigraphic sense, manganese appears in the stratigraphic column well before iron appears, and disappears well before iron disappears.

The manganese minerals typically occur as disseminated grains, mottles, lenses, and pods in iron-rich strata and as a pore-filling cement in quartz arenite. Manganese is most strongly concentrated in two zones in the iron-formation (Fig. 15) that more or less conform to the stratigraphic positions of the oolitic-pisolitic lithotope.

If we use an arbitrary cutoff grade of 10 percent manganese, the upper zone of strong manganese enrichment forms a stratabound lens, some 760 meters in strike length and as much as 15 meters thick, that occurs in the central part of the study area (Fig. 16). The lower zone of strong manganese enrichment is larger. It forms a stratabound lens that is locally as thick as 30 meters, although most of it is 15 to 18 meters thick. The lower zone pinches out to the east, but it can be traced with certainty along strike to the west for at least 1000 meters, and it can reasonably be inferred to continue to at least the west edge of section 20 for a total strike length of more than 1680 meters. However, the data imply that both the thickness of the zone

and manganese values within it decrease near the west edge of section 20. The chemical data (Tables 11 and 13), together with the partial analytical data for SiO_2, total Fe, and total Mn tabulated in the original exploration records, imply that both manganese-rich zones are composed of a series of lens-shaped masses containing 10-20 percent Mn, that are interspersed in less manganiferous rock. These lenses are composed of somewhat smaller lenses with 20-30 percent manganese that in turn consist of still smaller lenses about 1.5 to 3 meters thick and less than 30 meters long having values as high as 50 percent Mn. None of the small lenses seem to be stratigraphically constrained. This situation creates a problem when estimating grades and tonnage, because measured manganese values for any given set of samples are as much a function of the size of the stratigraphic interval over which the sample is taken as they are a function of the actual manganese content.

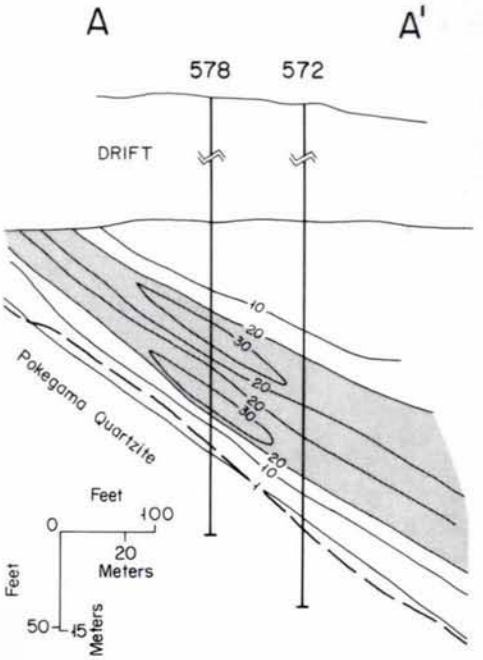

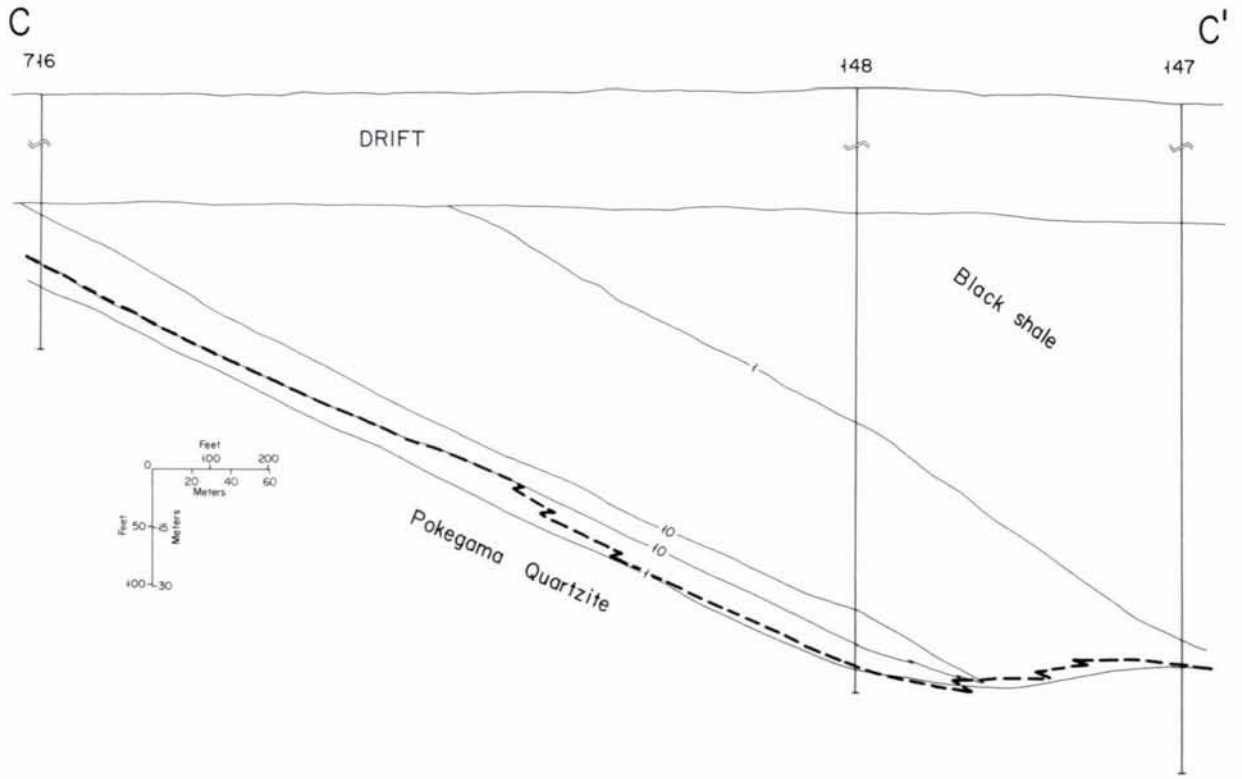

Figure 13. Selected longitudinal sections showing the inferred distribution of manganese in Unit A of Ruth Lake. See Figure 5 for locations. Contours in weight percent Mn.

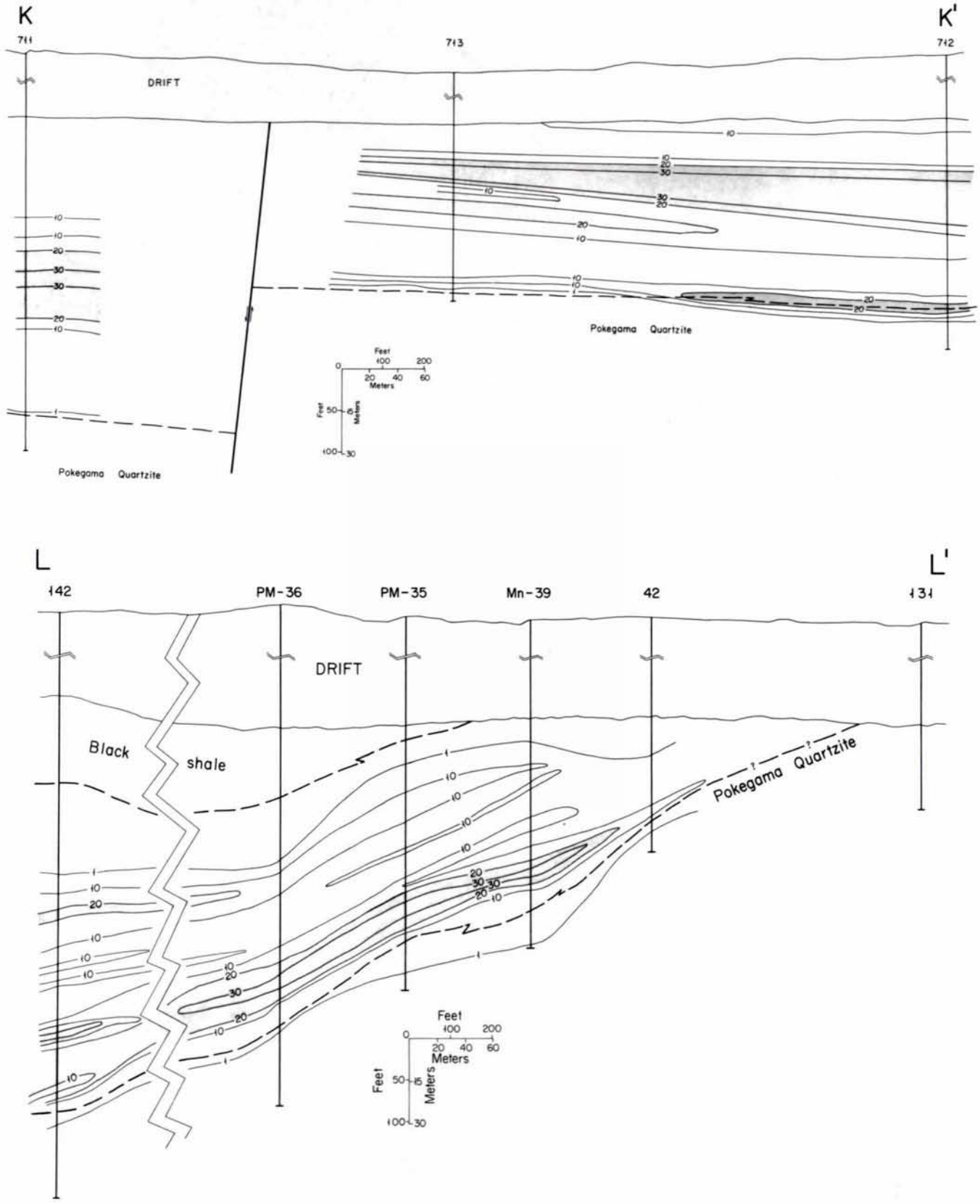

Figure 13. Continued

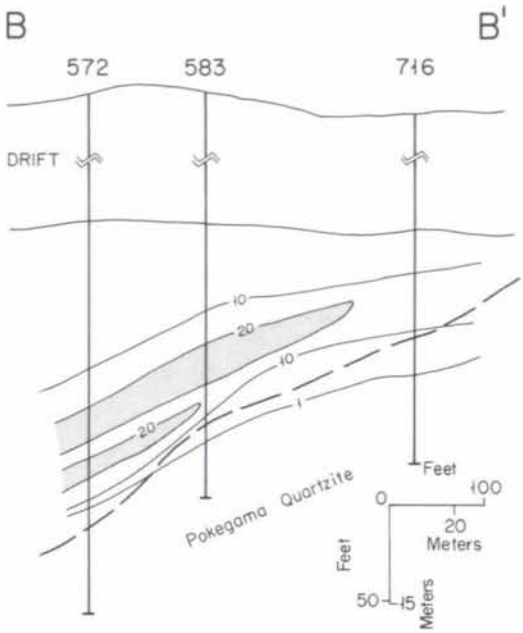

Figure 14. Selected cross sections showing the inferred distribution of manganese in Unit A of Ruth Lake. See Figure 5 for locations. Contours in weight percent Mn.

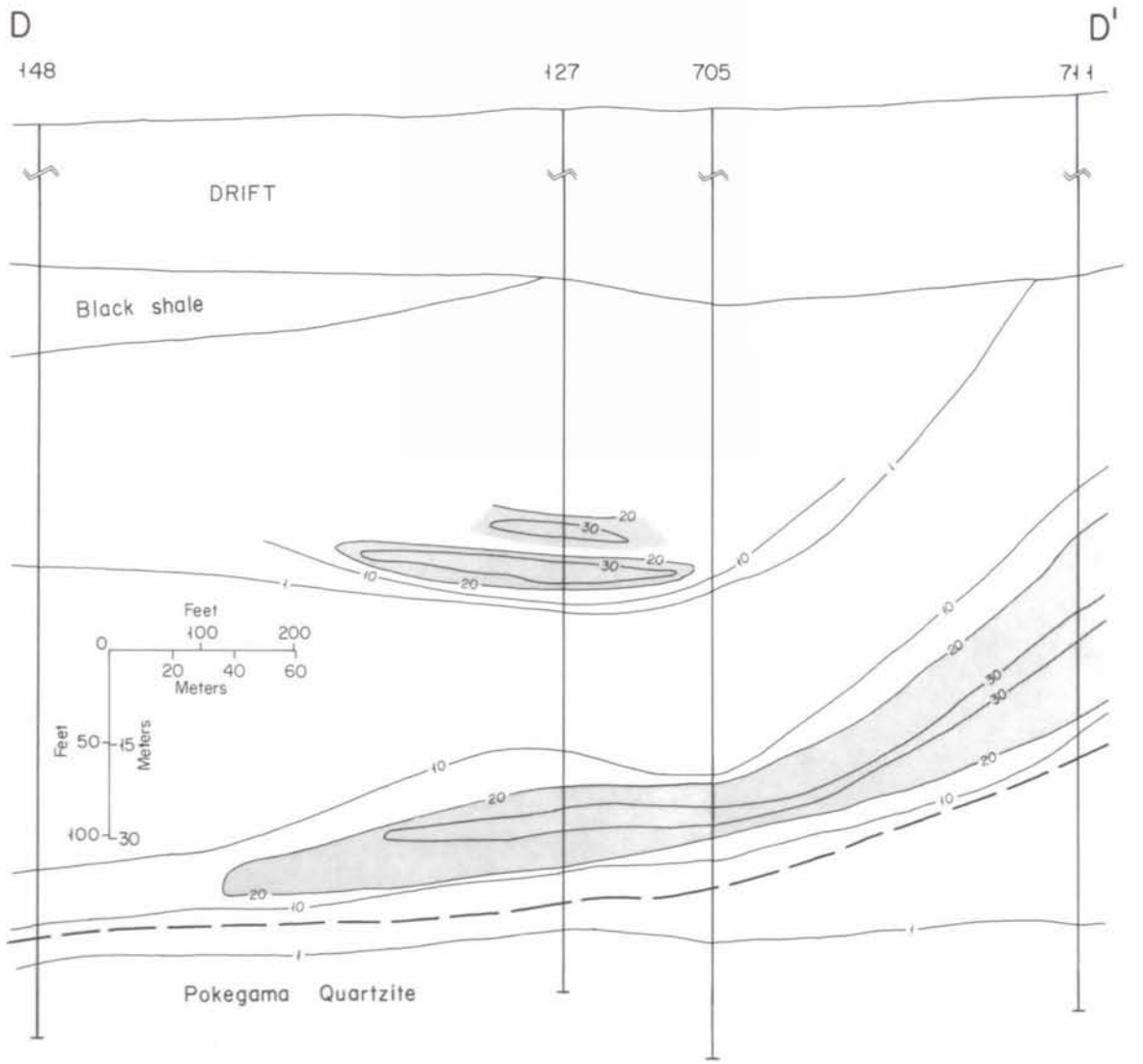

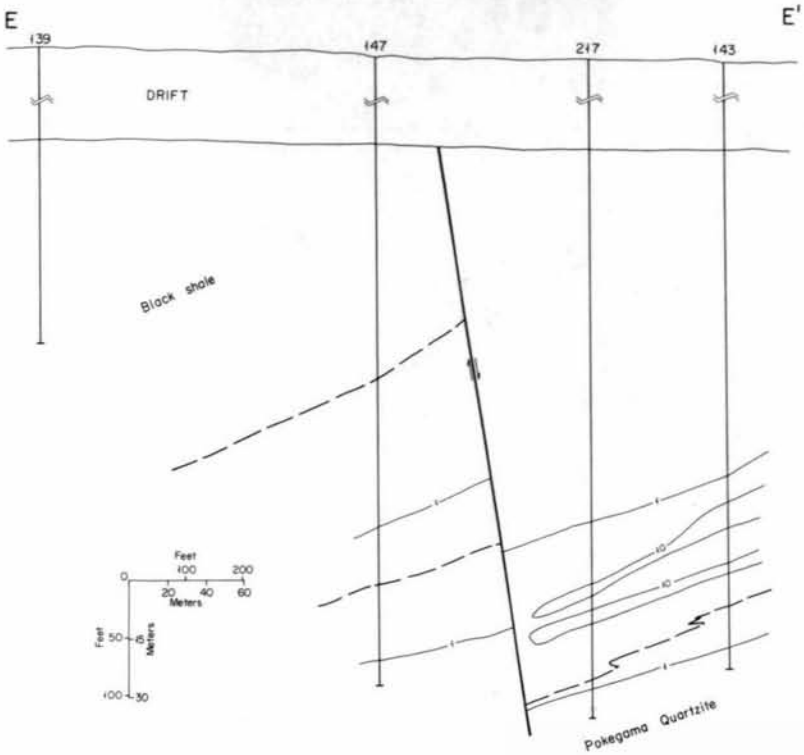

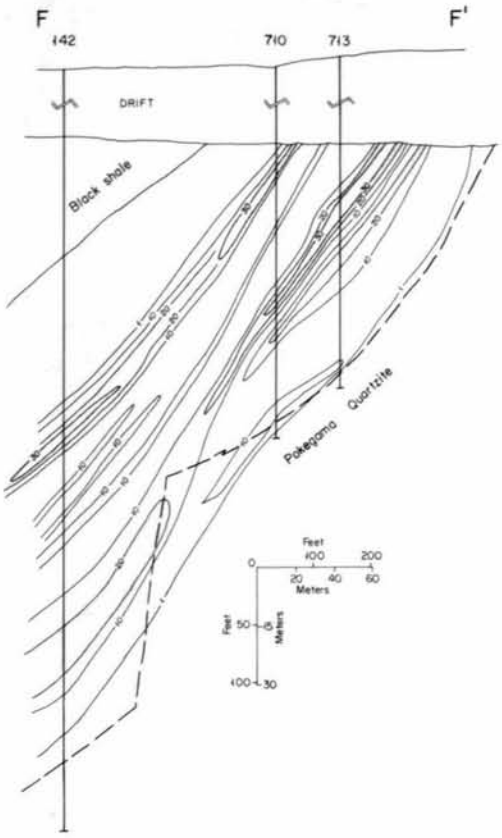

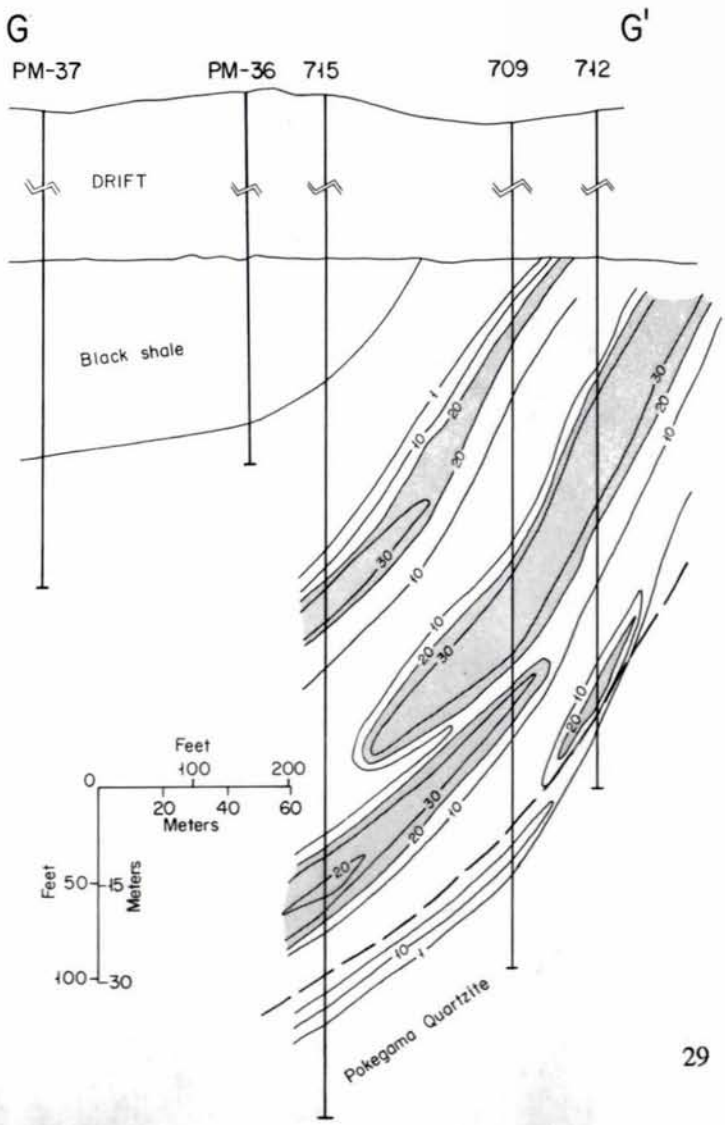

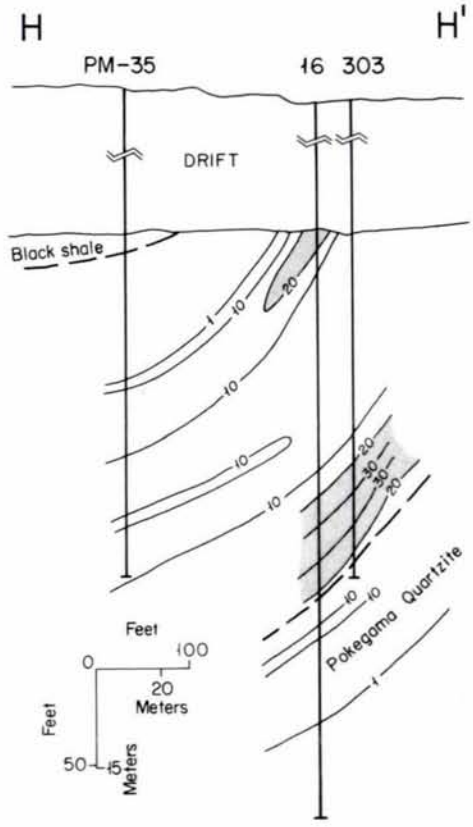

Figure 14. Continued

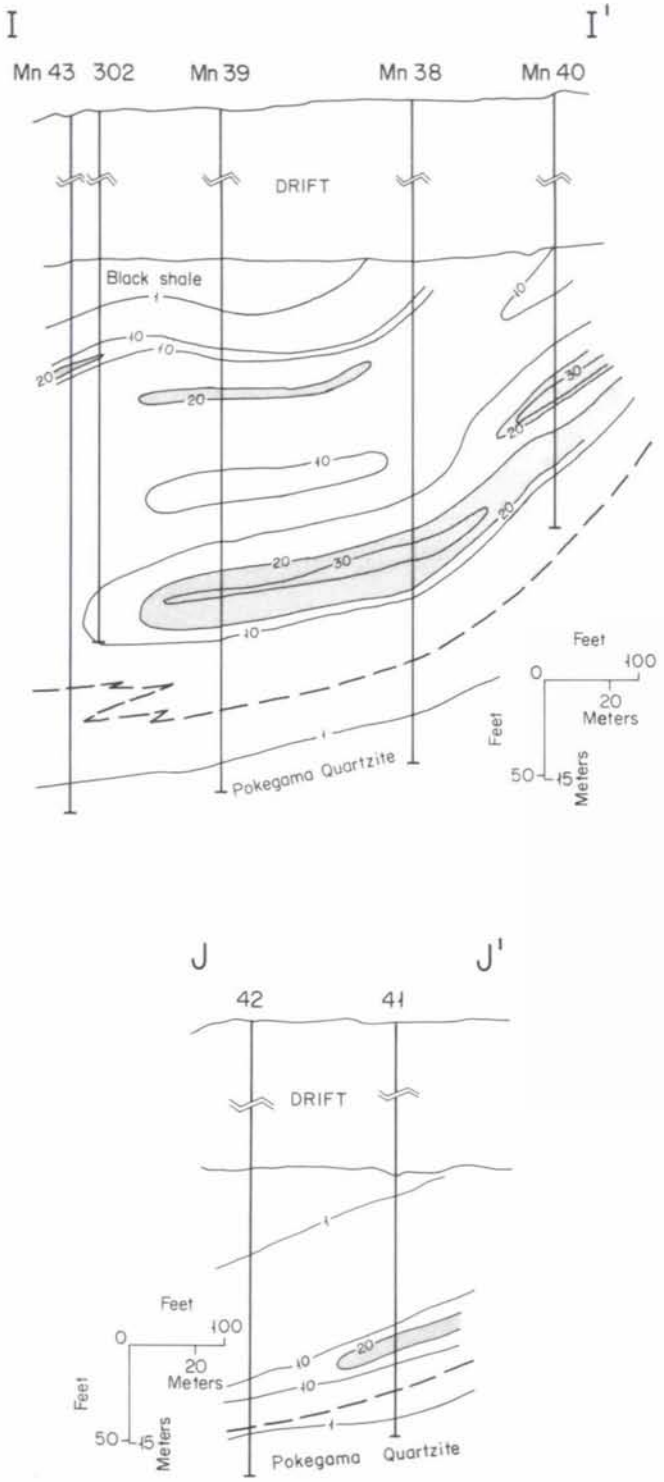

Figure 14. Continued

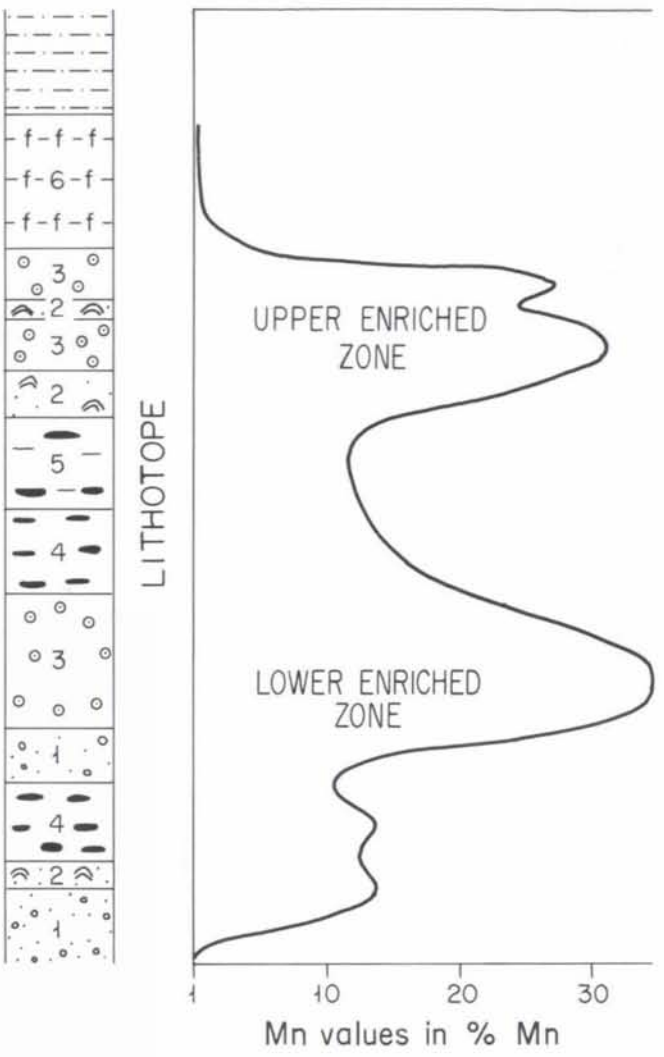

Figure 15. Diagram showing the vertical distribution of manganese (in weight percent Mn), as inferred from cross section G-G'. Note the presence of two enriched zones that more or less correspond to the stratigraphic positions of the oolitic/pisolitic lithotope.

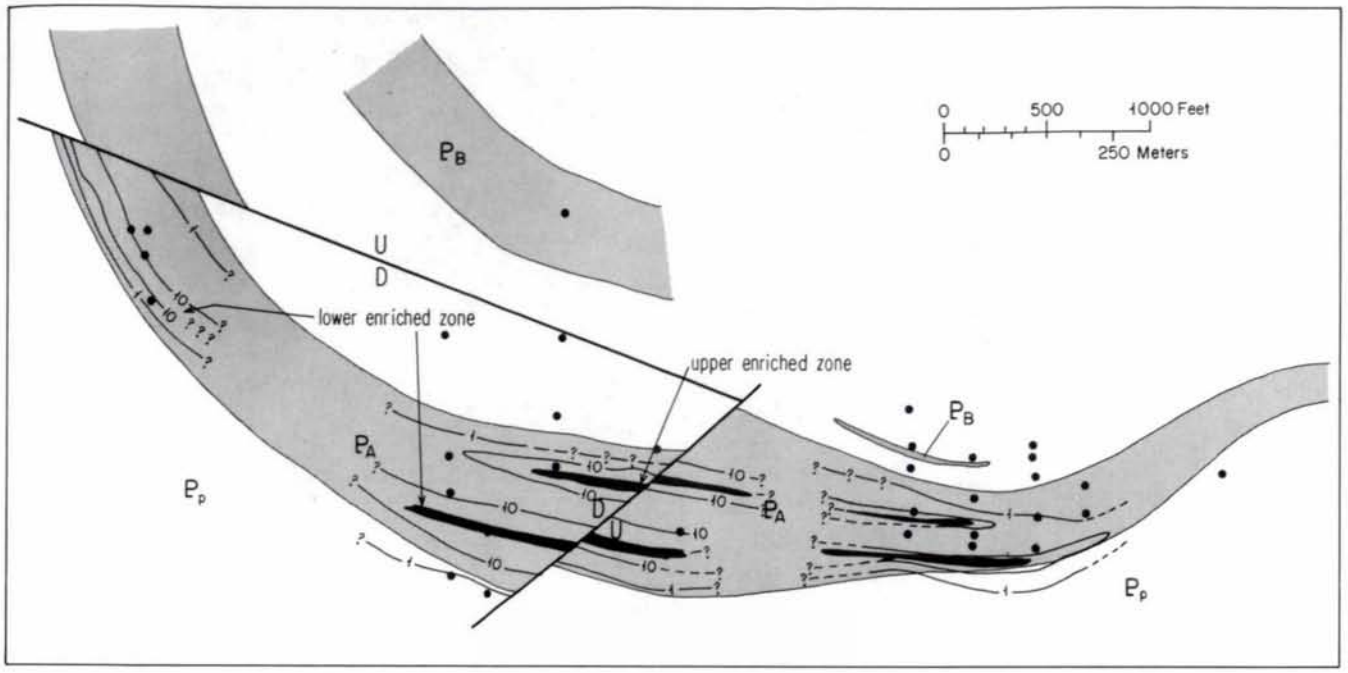

Figure 16. Geologic map of Unit A of the Ruth Lake area showing the inferred subcrop distribution of manganese-enriched zones. Contours at 1, 10, and >30% (black). manganese values.

Manganese minerals in both the upper and lower enriched zones are chiefly manganite, psilomelane, and cryptomelane (Tables 12 and 14). Pyrolusite also was identified from the lower zone, as was braunite, a manganese mineral believed to be of high-temperature origin. Although dominated by manganese oxides, both zones also contain appreciable quantities of goethite, hematite, and chert or quartz. Representative ratios of manganese to iron in the upper zone range from 0.43 to 1.55, and in the lower zone from 0.52 to 4.50.

Manganite appears to be the most abundant of the manganese minerals and is clearly of secondary origin in both enriched zones. It is difficult to determine the relative abundances of psilomelane and cryptomelane, which are probably primary, from X-ray diffraction data. The upper zone contains both potassium and barium (Table 13), consistent with the presence of both cryptomelane and psilomelane. The K_2O values of 0.13 to 0.17 percent are not unusual for iron-formation and are fundamentally the same as in the Biwabik Iron Formation of the Mesabi range. In contrast, the barium values of 0.69 to 0.86 percent in the upper zone greatly exceed those in the Biwabik, where barium occurs only in the parts per million range (average is about 26 ppm). These data imply that the barium-bearing phase may be the dominant manganese phase in the upper zone at Ruth lake.

As in the upper zone, it is difficult to determine from X-ray diffraction the relative abundance of cryptomelane and psilomelane in the lower zone. K_2O values (Table 11) ranging from 0.18 to 2.58 percent, imply that cryptomelane may be a fairly abundant phase. Similarly, samples from the lower zone containing 3.5 to 3.2 percent barium, imply that psilomelane also may be abundant.

In both enriched zones 83 to 93 percent consists chemically of silica, total iron as Fe_2O_3, total manganese as MnO, and alumina. Of these components, alumina is the least abundant, averaging 0.62 percent in the upper and 0.94 percent in the lower zone. These values differ very little on the average from those in the Biwabik Iron Formation where alumina ranges in value from 0.62 to 1.21 percent (Morey and Morey, 1990). Silica ranges in value from 10 to 48 percent, and manganese and iron oxides have combined totals ranging from 40 to nearly 80 percent. An inverse correlation exists between total Fe-Mn oxides and silica (Fig. 17), a predictable relationship given that (1) these three constituents dominate the samples that were analyzed, and (2) iron and manganese have similar chemical attributes and therefore should behave similarly in an oxic environment. However, Figure 18 shows that the relationship between silica, total iron, and total manganese is not perfectly straightforward. Total iron values, as measured over 1.5-meter stratigraphic intervals, tend to remain more or less

Table 11. Chemical analyses of selected samples from the lower enriched zone

Values in weight percent except as noted

Sample no.	(1)	(2)	(3)	(4)	(5)	(6)	(7)	(8)	(9)	(10)
Hole no.	142	572	572	572	572	572	709	711	711	578
Depth (ft.)	630	246	252	257a	275a	275b	390a	395b	407a	225
SiO_2	5.09	43.6	10.68	10.64	28.50	47.60	11.30	19.70	37.80	10.50
Al_2O_3	0.70	0.45	0.57	1.03	.94	0.82	1.76	1.17	0.73	1.89
TiO_2	321+	32+	656+	296+	124+	142+	410+	202+	224+	0.16
Fe_2O_3 Total	23.7	14.6	39.2	8.1	15.4	16.1	17.3	4.7	4.6	33.9
MnO	48.4	28.8	39.2	53.4	40.4	25.6	54.7	67.5	35.9	40.
MgO	0.11	940+	0.10	0.29	0.22	0.15	0.15	929+	0.19	0.12
CaO	0.19	1.13	0.26	6.78	0.15	0.17	0.42	1.89	3.83	0.21
Na_2O	713+	966+	0.25	0.17	654+	262+	1.14	0.15	0.14	0.29
K_2O	0.18	0.49	2.58	0.95	0.28	0.28	1.70	1.71	0.69	2.50
P_2O_5	0.19	0.32	0.20	0.45	0.11	0.16	0.71	0.98	0.16	0.92
CO_2	<.07	4.18	<.07	4.75	<.07	<.07	<.07	0.68	<.07	<.07
Sr	882+	596+	0.16	0.26	673+	379+	0.38	0.12	0.17	0.13
Ba	1.30	0.66	1.10	3.21	0.57	0.57	0. 33	0.32	0.70	0.95
				Values in ppm						
Hf	<4.	<6.	<6.	<3.	<5.	<5.	<4.	<66.	<4.	4.
Zr	29.	7.	52.	14.	19.	17.	48.	43.	7.8	90.
Y	45.7	17.3	66.2	80.3	38.7	60.3	56.5	36.9	21.4	70.1
Be	5.69	2.66	4.36	4.90	2.72	1.84	2.38	2.19	2.46	3.57
Zn	51.	36.	82.	76.	37.	33.	69.	46.	64.	67.
Cu	36.1	38.7	52.0	135.	238.	6.4	79.4	60.3	12.3	82.2
Sc	1.7	<.3	<.3	0.7	0.9	0.5	0.7	1.6	1.3	1.4
Co	128.	77.	125.	332.	76.	34.	93.	59.	68.	155.
Pb	<38.	<51.	<56.	<45.	<38.	<40.	<55.	<47.	<48.	<50.
Ni	32.	25.	49.	90.	26.	23.	72.	15.	37.	37.
Cr	<3.	4.	<4.0	<3.	<3.	<3.	4.	4.	<4.	<3.
Rb	<120.	<150.	<144.	<133.	<121.	<127.	<143.	<244.	<275.	<130.
V	6.	51.	37.	<4.	<3.	<3.	44.	67.	18.	22.
Ag	.032	.03	.002	.068	<.014	.02	.041	.044	.031	.016
As	111.	55.5	130.	59.0	101.	100.	59.6	84.1	59.3	100.
Au	.001	<.0005	<.0005	<.0005	.003	<.0005	<.0005	.0005	.001	.001
Hg	.542	.357	1.05	.499	.607	.436	.475	.346	.148	.706
Sb	.789	.277	.709	.325	.804	1.37	.797	8.35	<.246	.789

+ indicates values in parts per million

1. 142-630—Manganese-rich layer with a pisolitic and oolitic texture. A few of the pisolites and oolites seem to have cores of quartz. Ferruginous and manganiferous.
2. 572-246—Oolites and pisolites set in a coarse-grained matrix of intergrown chert, iron, and manganese oxides.
3. 572-252—Massive manganese-rich layer with considerable goethite.
4. 572-257a—Manganese-rich layer with little obvious goethite; intercalated with materials as in samples 572-246, 572-247, and 572-252.
5. 572-275a—Massive manganese-rich layer characterized in part by an oolitic texture with core grains of detrital quartz; intercalated with a manganiferous oolitic unit as represented by sample 572-256b.
6. 572-275b—Manganiferous oolites set in a matrix of granular quartz, manganese oxides, and iron oxides; intercalated with sample 572-275a.
7. 709-390a—Massive manganese-rich layer.
8. 711-395b—Manganese-rich layer, hard and structureless.
9. 711-407a—Manganese layers, massive, hard, and cut by scattered quartz veinlets.
10. 578-225—Pisolitic material, earthy, weathered; intercalated with beds of steely blue manganese oxides.

Table 12. Mineralogy of selected samples from the lower enriched zone

Sample no.	(1)	(2)	(3)	(4)	(5)	(6)	(7)	(8)	(9)	(10)	(11)	(12)	(13)	(14)	(15)
Hole no.	142	572	572	572	572	572	572	709	709	711	711	711	711	711	578
Depth (ft.)	630	246	252	257a	257b	275a	275b	390a	390b	379	395a	395b	407a	407b	225
Manganite	+	+	-	+	+	+	++	-	+	+	+	-	-	-	-
Pyrolusite	-	-	+	Tr	-	-	-	Tr	+	-	-	+	+	-	++
Psilomelane	Tr	+	+	+	+	Tr	+	++	++	-	++	++	+	-	+
Cryptomelane	+	+	+	+	+	+	+	+	+	-	+	+	+	-	+
Braunite	-	-	-	-	-	-	-	-	-	++	-	-	-	-	-
Hematite	+	+	+	Tr	-	+	+	-	-	+	+	-	+	+	+
Goethite	+	+	+	Tr	+	+	+	+	+	+	Tr	+	-	-	-
Quartz	+	+	-	-	-	-	-	-	+	+	-	-	+	++	-
Calcite	-	+	-	-	+	-	-	-	+	-	-	-	+	-	-
Siderite	+	-	-	+	-	-	-	-	-	-	-	+	-	-	-
10Å Mica	-	-	-	-	-	-	-	-	-	-	-	-	-	-	-
Kaolinite	-	-	-	-	-	-	-	-	-	-	-	-	-	+	-
Minnesotaite	+	-	-	+	+	-	+	-	-	-	-	-	-	-	-
Other (Amphibole)	-	-	-	-	-	-	-	-	-	-	+	-	-	-	-

++, abundant; +, present; Tr, trace; -, not observed.

1. 142-630—Manganese-rich layer with a pisolitic and oolitic texture. A few of the pisolites and oolites have cores of quartz and rims that are both ferruginous and manganiferous.
2. 572-246—Oolites and pisolites set in a coarse-grained matrix of intergrown chert, iron, and manganese oxides.
3. 572-252—Massive manganese-rich layer with considerable goethite.
4. 572-257a—Manganese-rich layer with little obvious goethite; intercalated with materials as in samples 372-246, 572-247, and 252.
5. 572-257b—Manganese- and goethite-rich layer; massive, hard, and black.
6. 572-275a—Manganiferous oolites set in a matrix of granular quartz, manganese oxides, and iron oxides; intercalated with sample 572-275a.
7. 572-275b—Massive manganese-rich layer; hard, metallic.
8. 709-390a—Massive manganese-rich layer; hard, metallic.
9. 709-390b—Same as 709-390a except for stong acid reaction of carbonate.
10. 711-379—Manganese and iron oxides coarsely intergrown with scattered grains of granular chert or detrital quartz.
11. 711-395a—Manganese-rich layer; hard and structureless with scattered grains of detrital quartz; interlayered with sample 711-395b.
12. 711-395b—Manganese-rich layer, hard and structureless.
13. 711-407a—Manganese-rich layer; massive, hard, and cut by scattered quartz veinlets.
14. 711-407b—Quartz veinlet cutting same as 711-407a.
15. 578-225—Pisolitic material, earthy and weathered.

Table 13. Chemical analyses of selected samples from the upper enriched zone

Values in weight percent except as noted

Sample no.	(1)	(2)	(3)
Hole no.	142	127	127
Depth (ft.)	420	350	380
SiO_2	10.5	21.7	36.9
Al_2O_3	0.54	0.42	0.90
TiO_2	401+	231+	0.12
Fe_2O_3 Total	11.0	36.3	24.2
MnO	63.0	29.8	29.8
MgO	0.11	0.22	428+
CaO	0.18	0.32	314+
Na_2O	905+	0.20	159+
K_2O	0.17	0.13	146+
P_2O_5	0.18	0.12	0.11
CO_2	<.07	<0.7	<.07
Sr	874+	0.14	.11+
Ba	.69	.86	121+
	Values in ppm		
Hf	<4	4	4
Zr	5.8	22	33
Y	15.9	33.3	21.5
Be	3.23	4.62	4.11
Zn	36.0	30.9	19.2
Cu	9.3	1.5	3.1
Sc	<.21	<.2	0.4
Co	33.0	144	14
Pb	234	<41	<41
Ni	13	21	13
Cr	4	7	6
Rb	<98	<129	<128
V	<3	37	52
Ag	.037	.029	.032
As	294.	28.8	13.2
Au	<.0005	.006	.02
Hg	.300	.354	.421
Sb	1.10	.513	.352

+ indicates values in parts per million

1. 142-420—See Table 14 for sample description.
2. 127-350—See Table 14 for sample description.
3. 127-380—See Table 14 for sample description.

Table 14. Mineralogy of selected samples from the upper enriched zone

Sample no.	(1)	(2)	(3)
Hole no.	142	127	127
Depth (ft.)	420	350	380
Manganite	++	++	++
Pyrolusite	-	-	-
Psilomelane	++	++	Tr
Cryptomelane	+	++	Tr
Braunite	-	-	-
Hematite	+	+	+
Goethite	-	+	+
Quartz	+	+	+
Calcite	-	Tr	-
Siderite	-	-	-
10Å Mica	-	-	-
Kaolinite	-	-	-
Minnesotaite	-	-	-
Other	-	-	-

++, abundant; +, present; Tr, trace; -, not observed

1. 142-420—Massive manganese-rich layer intercalated with sandy, granular, chert- and jasper-rich beds.
2. 127-350—Ferruginous and manganiferous, earthy; intercalated thick manganese-rich layers as in sample 127-380.
3. 127-380—Massive manganese-rich layer, earthy; contains scattered, round, sand-size grains of quartz; intercalated layers as in samples 127-350 and 127-400.

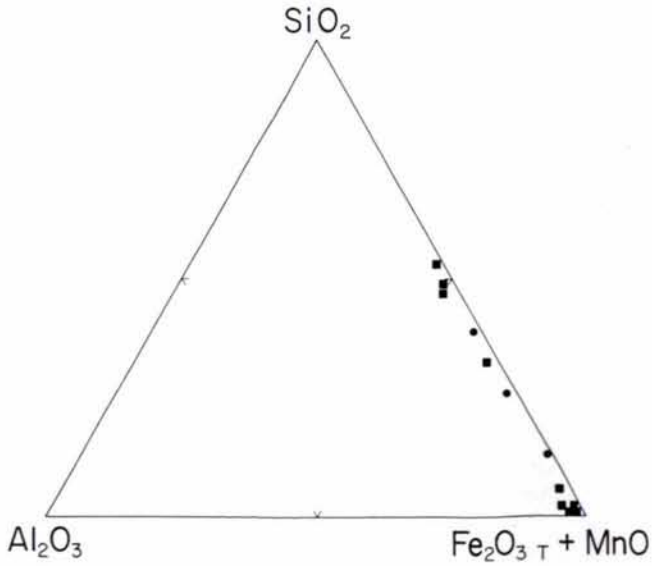

Figure 17. Silica—alumina—total iron and manganese oxide plot of the lower (squares) and upper (circles) enriched zones in Unit A.

constant in both iron-formation having ordinary Mn values and in zones highly elevated in Mn, but silica and manganese are inversely correlated. This implies that whatever processes were responsible for the precipitation of manganese in the enriched zones either inhibited the precipitation of silica or caused its dissolution in selected stratigraphic intervals.

Silica values in Unit A reflect the relative contributions of a chemically precipitated component, either chert or jasper, and a terrigenous component, most likely detrital quartz, and to a much lesser extent other silicate minerals of either terrigenous or volcanic origin. Thus to a first approximation, low silica values in the enriched zones could simply reflect a decline in any one or all of these components. Although of a very preliminary nature, rare earth element data (Table 15 and Fig. 19) reflect a dual source. Samples of chemically precipitated chert and jasper that were specifically selected to avoid any obvious terrigenous component appear to be depleted in rare earth elements and to have relatively flat distribution patterns. Furthermore, these samples are slightly enriched in Eu values, an attribute typical of many Early Proterozoic iron-formations (Fryer, 1983). Enriched Eu values have been interpreted as the result of hydrothermal input into the water from which the iron-formation precipitated (Fryer and others, 1979). If so, this input in the Ruth Lake area most likely reflects an aspect of the overall marine chemistry of the Animikie basin, because geologic evidence for a local volcanogenic or volcaniclastic contribution has not been recognized. In contrast, samples of quartz arenite from the epiclastic lithotope are relatively enriched in all the rare earth elements, especially the lighter elements. It seems likely that trace amounts of accessory minerals, such as zircon and apatite, control rare earth element distribution patterns in the epiclastic rocks. These accessory minerals seem to be concentrated in the sand-size detrital fraction, most likely by hydrologic processes related to grain size. This relationship is shown by the fact that interlayered shaly beds have rare earth element distribution patterns that plot midway between the chemically precipitated and terrigenous end members.

Samples of ordinary oxide-facies iron-formation are relatively enriched in all the rare earth elements, but particularly in the lighter elements. This pattern could reflect a terrigenous component, but the pattern is also broadly similar to that of a sample of Biwabik Iron Formation (Wildeman and Haskin, 1973) that lacks an obvious terrigenous component. In this regard, Fryer (1977) suggested that enriched rare earth elements in oxide-facies iron-formation could also reflect chemically precipitated materials that have undergone complex diagenetic changes.

Rare earth element patterns from the two zones of elevated Mn values are broadly similar to those described for other rock types that contain terrigenous materials, although somewhat reduced in absolute abundances. These patterns could reflect the fact that the oolitic-pisolitic lithotope contains an appreciable terrigenous component, but they also could reflect the highly oxidized nature of the sample materials. Regardless, the rare earth element patterns are of little value in reconstructing the diagenetic history of the Ruth Lake area.

PARAGENESIS OF THE MANGANESE ZONES AT RUTH LAKE

Because the rocks of the Emily district, including those at Ruth Lake, were pervasively oxidized during late Mesozoic weathering, it has not been possible to establish with certainty whether the iron and manganese oxides are syngenetic or epigenetic. Many of the stratigraphic and textural attributes of the Emily district iron-formations are very much like those in unoxidized magnetite-rich parts of the Biwabik Iron Formation. This similarity, coupled with the extensive occurrence of obviously secondary goethite and manganite in the Emily district, led Marsden (1972) to infer that the Emily rocks (including Unit A) were simply the oxidized equivalents of formerly magnetite-bearing strata of the Biwabik. This scenario, in our view, although consistent with much of the evidence, does not account for the abundance of manganese in the Emily district.

Any model that purports to account for elevated manganese values in the Ruth Lake area must also explain the following other observations. (1) The Ruth Lake sequence is an ordinary Animikian iron-formation which contains, except for manganese oxides, ordinary quantities of iron, silica, and other major-element constituents. (2) There is no substantial evidence that the manganese was deposited as carbonates or silicates that were later transformed, without trace, to oxides by weathering. Lacking solid evidence to the contrary, it is admissible to postulate that the manganese was precipitated as an oxide phase. (3) The iron and manganese oxides occupy overlapping but not identical stratigraphic intervals. Above-background values of manganese (1% Mn) first appear at Ruth Lake at a stratigraphic level well below that of the first appearance of chemically precipitated iron. Similarly, the iron oxides disappear from the sequence at a stratigraphic level well above that where manganese oxides disappear. (4) There are two stratigraphically constrained zones of elevated Mn content ($\geq$ 10% Mn) where an inverse correlation exists between silica and manganese. (5) The Mn-rich zones contain well above average values of barium, as compared to ordinary iron-formation.

These observations cannot be easily reconciled with a syngenetic model involving the co-precipitation of iron and manganese in an oxic environment. Any syngenetic depositional sequence should be characterized by a direct relationship between iron and manganese, because the two

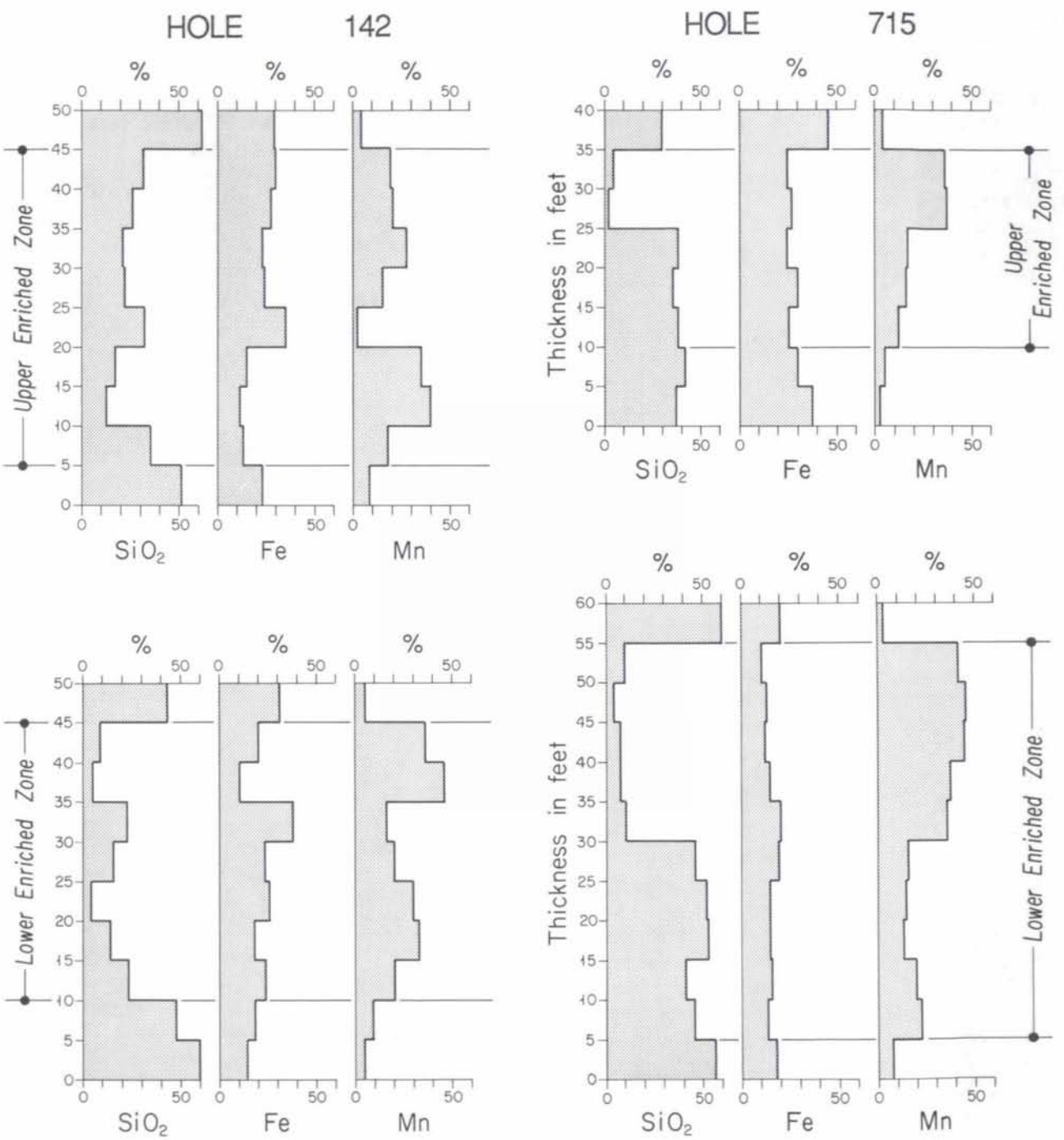

Figure 18. Graphs of stratigraphic distribution of silica, iron, and manganese values in the upper and lower enriched zones from two drill holes in the Ruth Lake area. Values based on the analyses of 1.5-meter (5-foot) intervals where Fe equals total iron and Mn total manganese.

Table 15. Rare earth analyses of selected samples from various lithotopes and enriched zones

[Values in ppm. Analyses by neutron activation methods, X-ray Assay Laboratories, Don Mills, Ontario]

Sample no.	(1)	(2)	(3)	(4)	(5)	(6)	(7)	(8)	(9)	(10)	(11)	(12)	(13)
Hole no.	142	127	127	572	572	572	572	709	709	711	142	572	709
Depth (ft.)	420	350	400a	246	275a	275b	293	345b	427	330	675a	325	450
La	53.8	27.	22.	2.9	1.23	0.4	1.33	0.20	128.	71.0	29.4	4.3	19.5
Ce	48.3	36.	27.	4.8	2.18	0.8	3.34	0.49	157.	102.	69.	9.	86.
Nd	11.3	14.	6.	1.0	0.53	<0.1	0.46	0.08	67.	50.	18.	3.	19.
Sm	16.3	17.	23.	5.3	1.91	0.7	2.29	0.33	10.2	7.9	3.0	0.5	3.5
Eu	47.5	79.	32.	6.2	2.31	1.2	4.77	0.72	4.04	2.63	1.27	0.20	1.31
Tb	37.1	59.	33.	6.8	2.69	1.4	4.39	0.65	1.5	1.1	0.6	<0.1	0.7
Yb	64.7	88.	34.	5.6	2.09	1.1	2.92	0.42	4.80	3.20	1.68	0.71	2.30
Lu	2.3	157.	67.	10.2	4.04	1.5	4.80	0.68	0.68	0.45	0.23	0.13	0.33

1. 142-420—Upper enriched zone; manganese-rich layer; intercalated thick beds of sandy, granular chert and thin beds of jasper.
2. 127-350—Upper enriched zone; ferruginous and manganiferous; earthy texture; intercalated thick manganese layers.
3. 127-400a—Jasper; in situ stromatolitic structures cemented by chert that contains scattered sand-size grains of quartz.
4. 572-246—Lower enriched zone; oolitic and pisolitic with a coarse-grained intergrown matrix of iron and manganese oxides.
5. 572-275a—Lower enriched zone; massive manganese-rich layer; intercalated beds of manganiferous materials with an oolitic texture.
6. 572-275b—Lower enriched zone; disseminated manganiferous material set in a matrix of granular chert.
7. 572-293—Oolitic bed; iron- and manganese-bearing oolites set in a matrix of granular chert and disseminated iron oxides.
8. 709-345b—Iron-formation; granular with disseminated manganese oxides.
9. 709-427—Oolitic bed; manganese-rich; set in a matrix of granular chert and disseminated iron oxides.
10. 711-330—Quartz arenite or granular chert, ferruginous; intercalated with manganese-rich beds in upper enriched zone.
11. 142-675a—Quartz arenite; rounded sand-size grains cemented by manganese and iron oxides.
12. 572-325—Slate, shale or argillite, ferruginous; locally contains scattered, rounded, sand-size grains of quartz; intercalated with quartz arenite.
13. 709-450—Quartz arenite; fine to medium sand-size grains cemented by manganese and iron oxides; thick bedded with shaly and oolitic partings.

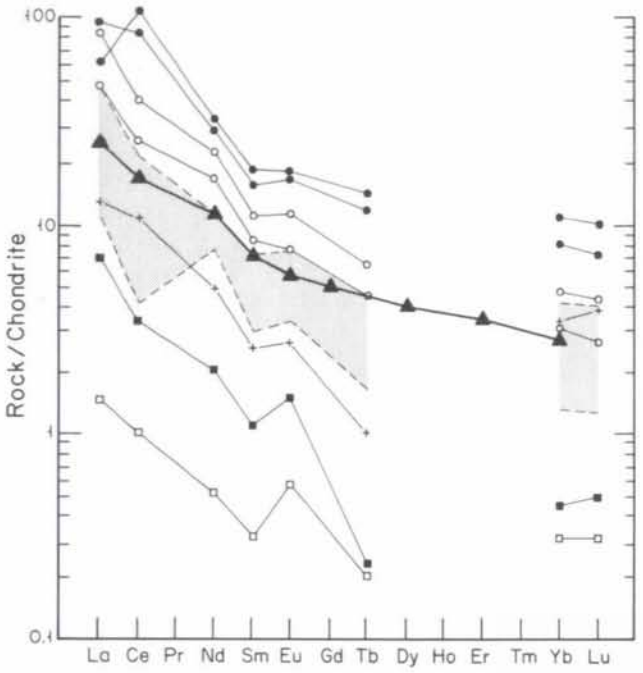

Figure 19. Plot of chondrite-normalized rare earth elements data from samples of various lithotopes in Unit A at Ruth Lake. The data are summarized in Table 15. •, quartz arenitic and +, shaly rocks of lithotope 1; ■, chert of lithotope 2; ○, lithotope 3; and □, chert of lithotope 6. Shaded areas enclose field of upper and lower enriched zones. ▲, Biwabik Iron Formation.

behave very similarly in an oxygen-rich environment (Hem, 1972). The only exception to this would be if iron was removed from the depositional system (as a sulfide, for example) before the manganese was precipitated (Cannon and Force, 1983; Force and Cannon, 1988), but this did not happen in the Ruth Lake area. It is also difficult to envision an oxic geochemical environment in which manganese oxides and barium are accumulating, and silica is being suppressed or dissolved. Given these problems with a simple syngenetic depositional model, we propose that the Ruth Lake sequence originated in two geochemical steps. The first process was the syngenetic precipitation of ordinary oxide-facies iron-formation in a shallow-water, oxic environment. The second was the epigenetic precipitation of manganese oxides at two stratigraphic levels by reflux processes involving anaerobic solutions carrying both manganese and barium. The refluxing is inferred to have happened relatively soon after primary sedimentation while the rocks were largely uncemented and porous.

The presence of manganese oxides in the coarser grained but not the finer grained parts of Unit A and their mode of occurrence within those coarser rocks are both consistent with an epigenetic origin. They occur as a pore-filling cement in the quartz arenitic parts of the epiclastic lithotope, and are fairly abundant in the granular parts of the iron-formation, but are all but lacking in non-granular parts. Lastly, the manganese oxides are most abundant in the oolitic and pisolitic lithotope, which on theoretical grounds would have had abundant primary porosity.

Primary porosity is not a feature normally attributed to Precambrian iron-formations. However LaBerge (1964) has pointed out that many of the granules in cherty or granular iron-formation are texturally akin to the fine-grained siltstone- or shale-like rock of slaty or non-granular iron-formation, and therefore might have been derived from such slaty units. Furthermore, granules commonly occur in strata that also have graded bedding, cross-bedding, intraformational conglomeratic clasts, algal structures, chert- or carbonate-pebble beds, as well as oolites, pisolites and sand-size grains of terrigenous quartz. All of these features imply that the granules behaved as reworked particulate detritus (Mengel, 1965). Therefore, the cherty or granular rocks have textural attributes similar to those of oolitic and intraclastic limestones of Phanerozoic age (Dimroth, 1968), which have an appreciable primary porosity (Folk, 1968).

Even though many granular iron-formations may have originally had a large primary porosity, Dimroth and Chauvel (1973) and Simonson (1987), among others, have shown that lithification starts very soon as evidenced by a general lack of compaction features. Evidence of compaction also is lacking at Ruth Lake, implying that there too, lithification was a very early diagenetic phenomenon (Dimroth, 1976). The lithification of a typical granular or cherty iron-formation generally involves the loss of pore water and the growth of a pore-filling cement. In hematite-facies rocks, that cement is mostly silica (Dimroth, 1977). However the inverse relationship between the amounts of silica and manganese in the two enriched zones at Ruth Lake implies that manganese oxides formed early in the paragenetic sequence and that their presence inhibited the subsequent precipitation of a silica cement. Thus we take the inverse relationship between silica and manganese as evidence that the latter formed very early in the epigenetic history of the strata.

The presence of barium at levels well above background in the manganese oxides is evidence for transport under anaerobic conditions. In normal aerobic marine waters, barium is buffered to very low concentrations by the mineral barite, whose stability is controlled by the presence of the sulfate anion. In anaerobic waters however, sulfur occurs as the sulfide rather than the sulfate anion and therefore would not be available to form barite. Thus elevated barium values in the Ruth Lake sequence imply that barium was introduced

by anaerobic waters in which the sulfate anion could neither form nor remain to any significant extent. Furthermore, the occurrence together of barium and manganese implies that both were carried to their final depositional site by the same anaerobic water system and that both were precipitated when the anaerobic water met and mixed with aerated water in uncemented iron-formation on the seafloor.

In summary, we suggest that a locally driven reflux model like that in Figure 20 can account for the manganiferous materials in the iron-formation of Unit A at Ruth Lake. Although it cannot be established with certainty, the model assumes that folded and fractured strata of the North range group were the source of the manganese. There the Trommald Formation contains from 5 to more than 15 percent manganese, mainly as a carbonate (Schmidt, 1963), and is intercalated with fine-grained rocks that are in part carbonaceous. Fractures and steeply inclined bedding planes provided pathways along which anaerobic solutions could form, migrate, and selectively dissolve manganese, as well as other constituents. Manganese was selectively removed because it is considerably more soluble than iron in the Eh-pH range of ground-water systems of this kind (Krauskopf, 1956). Furthermore, under extremely anaerobic conditions, ferrous sulfide is much more insoluble than any naturally occurring manganese analog. Thus manganese is effectively concentrated over iron in anaerobic ground-water systems. The model further assumes that the anaerobic ground water transported dissolved manganese to places beneath the Ruth Lake sediment-water interface where, upon mixing with oxidizing pore waters, manganese oxides were precipitated. In detail it would be expected that the anaerobic and aerobic solutions would meet and commingle in porous and permeable rock below the water-sediment interface. All of this is taken to indicate that the manganese oxides formed very early in the epigenetic history of the strata at Ruth Lake.

RESOURCE ESTIMATION

No formal estimate has yet been made of the manganese resource in the Ruth Lake area. However the two enriched zones could contain 1 to 2 million metric tons of material averaging at least 20 percent Mn. Manganese also occurs in other parts of the Emily district. The so-called Emily-Shawmut Reserve in section 5, T. 137 N., R. 26 W. contains 515,000 tons of material averaging 11.50 percent manganese, and an additional 402,000 tons averaging 9.32 percent manganese (file data, Minnesota Department of Taxation, Office of Ore Estimation). Other localities in the township also contain at least 924,000 tons of material averaging 10.56 percent manganese. Thus the Emily district contains a large, but poorly quantified manganese resource.

Although the resource is large, no serious consideration has been given to economically recovering the manganese.

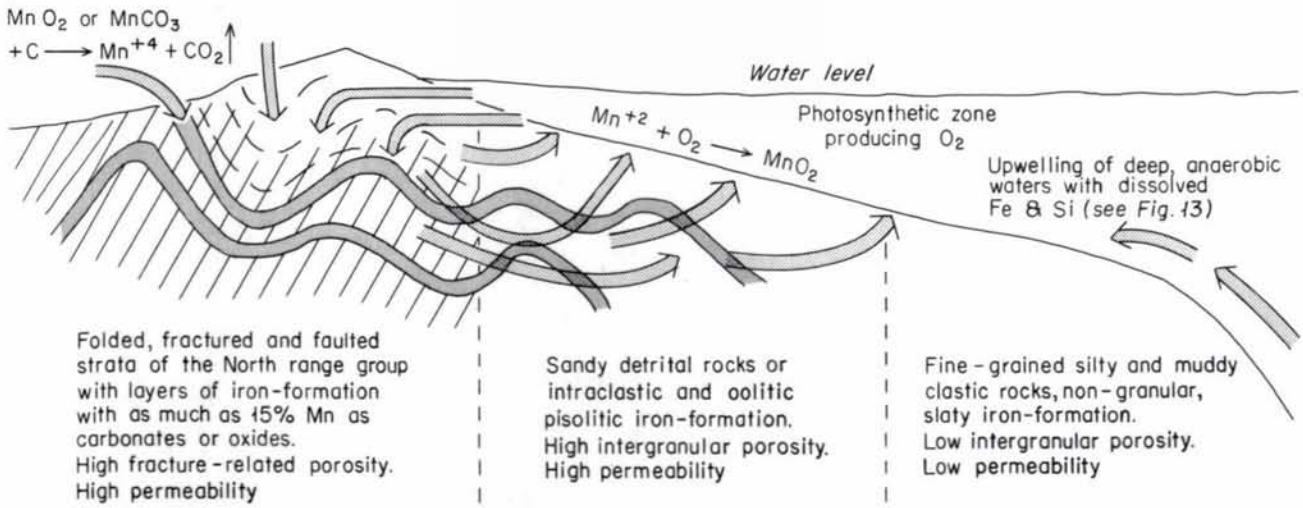

Figure 20. Schematic interpretation of manganese precipitation in Unit A by a reflux mobilization model (modified from Zajac, 1972 as reported by Dimroth, 1976). Manganese is mobilized by the dissolution of manganese oxides or carbonates in strata of the North range as reducing solutions migrate basinward. The manganese is reprecipitated at or very close to the sediment-water interface where the reducing solutions encounter oxidizing conditions.

The enriched zones at Ruth Lake are deeply buried (55-60 meters) for their size, and therefore open-pit mining may not be feasible. Furthermore, because the enriched zones have a tabular, near-horizontal configuration, it seems likely that they cannot be easily extracted by underground mining techniques. However, the main problem with these, and Cuyuna ores in general, involves the large amount of energy that must be expended to separate the manganese from the iron. Because of the costs, the more or less standard beneficiation techniques that were utilized in the past on the Cuyuna range were economically feasible only with government support in times of national emergency.

The abundance of manganese in stratabound zones makes the Ruth Lake area a candidate for innovative mining technology, such as the in situ techniques currently being developed by the U.S. Bureau of Mines and the Mineral Resources Research Center of the University of Minnesota. However if in situ mining is to be successful, considerable care must be taken to design metallurgical and beneficiation techniques that are specifically matched to a particular mineral system. And in today's world, the new techniques must be acceptable environmentally. These research challenges must be met before the Emily manganese resource can be classified as a reserve.

ACKNOWLEDGMENTS

This project was supported in part by the basic research component of the Mineral Diversification Program as administered by the Minerals Coordinating Committee for the Minnesota State Legislature. The Minnesota Department of Natural Resources, Division of Minerals at Hibbing, provided access to core materials and other exploration records which underpin much of this work. The U.S. Bureau of Mines Twin Cities Research Center, in Minneapolis, and Mr. Steve Carlton of Emily, Minnesota, provided additional exploration records, core materials, and interesting discussion.

REFERENCES CITED

Bath, G.D., Schwartz, G.M., and Gilbert, F.P., 1964, Aeromagnetic and geologic map of east-central Minnesota: U.S. Geological Survey Geophysical Investigations Map GP-474, scale 1:250,000.

_____1965, Aeromagnetic and geologic map of west-central Minnesota: U.S. Geological Survey Geophysical Investigations Map GP-473, scale 1:250,000.

Beltrame, R.J., Holtzman, R.C., and Wahl, T.E., 1981, Manganese resources of the Cuyuna range, east-central Minnesota: Minnesota Geological Survey Report of Investigations 24, 22 p.

Cannon, W.F., and Force, E.R., 1983, Potential for high-grade shallow-marine manganese deposits in North America, *in* Shanks, W.C., III, ed., Cameron volume on unconventional mineral deposits: New York, Society of Mining Engineers of the American Institute of Mining, Metallurgical, and Petroleum Engineers, p. 175-189.

Carlson K.E., 1985, A combined analysis of gravity and magnetic anomalies in east-central Minnesota: Unpublished M.S. thesis, University of Minnesota, Minneapolis, 138 p.

Chandler, V.W., 1983a, Aeromagnetic map of Minnesota, St. Louis County: Minnesota Geological Survey Aeromagnetic Map Series A-2, scale 1:250,000, 2 pls.

_____1983b, Aeromagnetic map of Minnesota, Carlton and Pine Counties: Minnesota Geological Survey Aeromagnetic Map Series A-3, scale 1:250,000, 2 pls.

_____1983c, Aeromagnetic map of Minnesota, east-central region: Minnesota Geological Survey Aeromagnetic Map Series A-4, scale 1:250,000, 2 pls.

_____1985, Aeromagnetic map of Minnesota, central region: Minnesota Geological Survey Aeromagnetic Map Series A-5, scale 1:250,000, 2 pls.

Chandler, V.W., and Malek, K.C., 1991, Moving-window Poisson analysis of gravity and magnetic data from the Penokean orogen, east-central Minnesota: Geophysics, v. 56, p. 123-132.

Dimroth, E., 1968, Sedimentary textures, diagenesis and sedimentary environment of certain Precambrian ironstones: Neues Jahrbuch für Geologie und Päleontologie Abhandlungen, v. 130, p. 247-274.

_____1976, Aspects of the sedimentary petrology of cherty iron-formation, *in* Wolf, K.H., ed., Handbook of stratabound and stratiform ore deposits: Amsterdam, Elsevier, v. 7, p. 203-254.

_____1977, Facies models 6, diagenetic facies of iron-formation: Geoscience Canada, v. 4, p. 83-88.

Dimroth, E., and Chauvel, J.J., 1973, Petrography of the Sokoman Iron Formation in part of the central Labrador trough, Quebec, Canada: Geological Society of America Bulletin, v. 84, p. 111-134.

Eugster, H.P., and Chou, I.M.,1973, The depositional environment of Precambrian banded iron-formations: Economic Geology, v. 68, p. 1114-1168.

Ewers, W.E., 1983, Chemical factors in the deposition and diagenesis of banded iron-formation, *in* Trendall, A.F., and Morris, P.C., eds., Iron-formation: Facts and problems: Amsterdam, Elsevier, p. 491-512.

Folk, R.L., 1968, Petrology of sedimentary rocks: Austin, Texas, Hemphill's Book Store, 170 p.

Force, E.R., and Cannon, W.F., 1988, Depositional model for shallow-marine manganese deposits around black shale basins: Economic Geology, v. 83, p. 93-117.

Fryer, B.J., 1977, Rare earth evidence in iron-formations for changing Precambrian oxidation states: Geochimica et Cosmochimica Acta, v. 41, p. 361-367.

_____1983, Rare earth elements in iron-formation: Facts and Problems: Amsterdam, Elsevier, p. 345-358.

Fryer, B.J., Fyfe, W.S., and Kerrich, R., 1979, Archean volcanogenic oceans: Chemical Geology, v. 24, p. 25-33.

Goodwin, A.M., 1956, Facies relations in the Gunflint iron formation: Economic Geology, v. 51, p. 565-595.

Grout, F.F., and Wolff, J.F., Sr., 1955, The geology of the Cuyuna District, Minnesota: A progress report: Minnesota Geological Survey Bulletin 36, 144 p.

Harder, E.C., and Johnston, A.W., 1918, Preliminary report on the geology of east-central Minnesota, including the Cuyuna iron-ore district: Minnesota Geological Survey Bulletin 15, 178 p.

Hem, J.D., 1972, Chemical factors that influence the availability of iron and manganese in aqueous systems: Geological Society of America Special Paper 140, p. 17-24.

Hoffman, P.F., 1987, Early Proterozoic foredeeps, foredeep magmatism, and Superior-type iron-formations of the Canadian shield, *in* Kröner, A., ed., Proterozoic lithospheric evolution: American Geophysical Union Geodynamics Series, v. 17, p. 85-98.

James, H.L., 1955, Sedimentary facies of iron-formation: Economic Geology, v. 49, p. 235-293.

Keighin, C.W., Morey, G.B., and Goldich, S.S., 1972, East-central Minnesota, *in* Sims, P.K., and Morey, G.B., eds., Geology of Minnesota: A centennial volume: Minnesota Geological Survey, p. 240-255.

Krauskopf, K.B., 1956, Dissolution and precipitation of silica at low temperatures: Geochimica et Cosmochimica Acta, v. 10, p. 1-26.

Krenz, K.A., and Ervin, C.P., 1977, Simple Bouguer gravity map of Minnesota, Duluth sheet: Minnesota Geological Survey Miscellaneous Map M-37, scale 1:250,000.

LaBerge, G.L., 1964, Development of magnetite in iron formations of the Lake Superior region: Economic Geology, v. 59, p. 1313-1342.

Lepp, H., 1966, Chemical composition of Biwabik Iron Formation, Minnesota: Economic Geology, v. 61, p. 243-250.

_____1968, Distribution of manganese in Animikian iron formations of Minnesota: Economic Geology, v. 63, p. 61-75.

_____1987, Chemistry and origin of Precambrian iron-formations, *in* Appel, P.W.U., and LaBerge, G.L., eds., Precambrian iron-formations: Athens, Greece, Theophrastus Publications, p. 3-30.

Lepp, H., and Goldich, S.S., 1964, Origin of Precambrian iron formations: Economic Geology, v. 59, p. 1025-1060.

Markello, J.R., and Reed, J.F., 1981, Carbonate ramp-to-deeper shelf transitions of an upper Cambrian intrashelf basin, Nolichucky Formation, Southwest Virginia Appalachians: Sedimentology, v. 28, p. 573-597.

Marsden, R.W., 1972, Cuyuna district, *in* Sims, P.K., and Morey, G.B., eds., Geology of Minnesota: A centennial volume: Minnesota Geological Survey, p. 227-239.

McGinnis, L.D., Carlson, D.R., Pederson, R., and Schafersman, J.S., 1977, Simple Bouguer gravity map of Minnesota, Stillwater sheet: Minnesota Geological Survey Miscellaneous Map M-35, scale 1:250,000.

McGinnis, L.D., Jackson, J.K., and Ervin, C.P., 1978, Simple Bouguer gravity map of Minnesota, Brainerd sheet: Minnesota Geological Survey Miscellaneous Map M-40, scale 1:250,000.

Mengel, J.T., Jr., 1965, Precambrian taconite iron formation: A special type of sandstone [abs.]: Geological Society of America, 79th Annual Meeting, Kansas City, Missouri, 1965, Program, p. 106.

Morey, G.B., 1978, Lower and Middle Precambrian stratigraphic nomenclature for east-central Minnesota: Minnesota Geological Survey Report of Investigations 21, 52 p., 1 pl.

_____1983, Lower Proterozoic stratified rocks and the Penokean orogeny in east-central Minnesota, *in* Medaris, L.G., Jr., ed., Early Proterozoic geology of the Lake Superior region: Geological Society of America Memoir 160, p. 97-122.

Morey, G.B., and Morey, P.R., 1990, Major and minor element chemistry of the Biwabik Iron Formation and associated rocks, Minnesota, *in* AIME, Minnesota Section, 63rd Annual Meeting, and Mining Symposium, 51st, 1990, Minnesota, Proceedings: University of Minnesota, Duluth, Continuing Education and Extension, Center for Professional Development, p. 259-287.

Morey, G.B., Olsen, B.M., and Southwick, D.L., 1981, Geologic map of Minnesota, east-central Minnesota, bedrock geology: Minnesota Geological Survey, scale 1:250,000.

Schmidt, R.G., 1963, Geology and ore deposits of Cuyuna North range, Minnesota: U.S. Geological Survey Professional Paper 407, 96 p.

Siever, R., 1962, Silica Solubility, 0-200° C, and the diagenesis of siliceous sediments: Journal of Geology, v. 70, p. 127-150.

Simonson, B.M., 1987, Early silica sedimentation and subsequent diagenesis in arenites from four Early Proterozoic iron-formations of North America: Journal of Sedimentary Petrology, v. 57, p. 494-511.

Southwick, D.L., Morey, G.B., and McSwiggen, P.L., 1988, Geologic map (scale 1:250,000) of the Penokean orogen, central and eastern Minnesota, and accompanying text: Minnesota Geological Survey Report of Investigations 37, 25 p., 1 pl.

Walter, M.R., Bauld, J., and Brock, J.D., 1972, Siliceous and bacterial stromatolites in hot springs and geyser effluents of Yellowstone National Park: Science, v. 178, p. 404-405.

White, D.A., 1954, Stratigraphy and structure of the Mesabi range, Minnesota: Minnesota Geological Survey Bulletin 38, 92 p.

Wildeman, T.R., and Haskin, L.A., 1973, Rare earths in Precambrian sediments: Geochimica et Cosmochimica Acta, v. 37, p. 419-438.

Woyski, M.S., 1949, Intrusives of central Minnesota: Geological Society of America Bulletin, v. 62, p. 999-1016.

Zapffe, C., 1933, The Cuyuna iron-ore district: International Geological Congress Guidebook 27, Excursion C-4, Lake Superior region, p. 72-88.

Zajac, I.S., 1972, The stratigraphy and mineralogy of the Sokoman Formation in the Knob Lake area, Quebec and Newfoundland: Unpublished Ph.D. dissertation, University of Michigan, Ann Arbor, 271 p.